atmosphere

MDPI

Article

Assessing COVID-19 Pandemic-Induced Air Quality Improvements: Insights from Marienplatz in Stuttgart, Germany

Abdul Samad [1,*], Macdonald Nwamuo [1,2], Godfrey Omulo [3], Frederick Nwanganga [4] and Ulrich Vogt [1]

[1] Institute for Energy Process Engineering and Dynamics in Energy Systems (IED), University of Stuttgart, 70569 Stuttgart, Germany
[2] Spiraltec GmbH, 74343 Sachsenheim, Germany
[3] Institute of Agricultural Sciences in the Tropics, University of Hohenheim, 70599 Stuttgart, Germany
[4] Mendoza College of Business, University of Notre Dame, Notre Dame, IN 46556, USA
* Correspondence: abdul.samad@ied.uni-stuttgart.de

Abstract

This study provides a comprehensive assessment of the impacts of COVID-19 pandemic-induced lockdowns on urban air quality at Marienplatz in Stuttgart, Germany, from 2018 to 2022. Utilizing high-resolution temporal datasets and advanced analytical techniques, including meteorological normalization and Shapley Additive Explanations (SHAP), the research disentangles the effects of emission reductions from meteorological variability on key atmospheric pollutants (CO, NO, NO_2, O_3, PM2.5, PM10). The findings reveal that the lockdown phases resulted in pronounced and significant reductions in primary traffic-related pollutants, with CO and NO concentrations declining by more than 50% relative to pre-pandemic baselines. In contrast, secondary pollutants, notably ozone, exhibited substantial increases (up to 50%), attributable to altered photochemical regimes and reduced NO_x titration, as confirmed by O_x-NO_x relationship analyses and photochemical sensitivity diagnostics. Particulate matter trends revealed limited short-term response, indicating persistent contributions from non-traffic sources such as residential heating and regional transport. Meteorologically normalized trends and SHAP analyses further confirmed that emission reductions, rather than meteorological fluctuations, were the primary drivers of the observed improvements in air quality. These insights highlight the transient and pollutant-specific nature of air-quality responses to abrupt emission reductions and provide critical scientific evidence to inform the design of robust, multi-sectoral urban air quality management and climate adaptation strategies in the post-pandemic era.

Keywords: COVID-19 lockdown; air quality; air pollutants; urban air pollution; stationary monitoring station; Marienplatz; Stuttgart

Academic Editor: Alexandra Monteiro

Received: 6 February 2026
Revised: 6 March 2026
Accepted: 9 March 2026
Published: 14 March 2026

1. Introduction

Air pollution remains one of the most critical environmental and public health crises worldwide, particularly in densely populated urban areas where industrial activities, vehicular emissions, and energy consumption converge [1]. According to the World Health Organization (WHO), over 90% of the global urban population is exposed to air pollution levels that exceed recommended thresholds, contributing to approximately seven million premature deaths annually [1]. The severity of air pollution varies significantly between developed and developing nations, primarily due to differences in regulatory frameworks, technological advancements, and economic priorities [2].

In developing countries, rapid urbanisation, industrial expansion, and reliance on low-quality fuels for cooking and transportation contribute to hazardous pollution levels [3]. Cities like Delhi, Dhaka, and Lagos frequently experience extreme concentrations of Particulate Matter (PM2.5, PM10), nitrogen dioxide (NO_2), and sulphur dioxide (SO_2), often exceeding WHO guidelines by five to ten times [4]. By contrast, developed nations have significantly reduced emissions through stringent environmental regulations, cleaner energy transitions, and advanced vehicular technologies [5]. However, persistent pollution from traffic, residential heating, and secondary pollutants such as ozone (O_3) continues to pose challenges in cities across Europe and North America [6].

Recent technological advancements, including low-cost sensor networks, satellite remote sensing, and AI-driven predictive models, have improved air quality monitoring by enabling real-time pollution tracking and more refined source apportionment [7,8]. Mitigation strategies such as electric-vehicle adoption, low-emission zones (LEZs), and green urban planning have been widely implemented in many cities globally [9]. Despite these advancements, several critical challenges persist: (i) the non-linear responses of pollutants to policy measures, where air quality improvements do not necessarily scale proportionately with regulatory measures due to complex atmospheric, economic, and behavioural factors (e.g., diesel emissions scandals in Europe) [10], (ii) emerging concerns over ultrafine particles (UFPs) and black carbon (BC), which remain underregulated despite their high toxicity [11], and (iii) climate change interactions, particularly the exacerbation of ground-level O_3 formation under rising temperatures [12].

The European Union (EU) has enacted some of the world's strictest air quality standards under the Ambient Air Quality Directive (2008/50/EC) [13]. However, many EU cities, particularly in Southern and Eastern Europe, continue to exceed NO_2 and PM limits [14]. The revised regulations, which will come into force in 2030, include legally binding reductions for PM2.5, P10, and NO_2, aligning EU thresholds more closely with WHO recommendations [15]. Despite its comparatively strong environmental policies, Germany continues to struggle with traffic-related NO_2 pollution [16], while particulate matter (PM) levels remain a persistent health concern, often due to continued reliance on diesel vehicles whose real-world emissions exceed regulatory expectations [16,17].

Cities like Munich, Berlin, and Stuttgart frequently experience elevated pollutant concentrations [18]. Stuttgart, located within a topographical basin, suffers from restricted air dispersion, leading to severe winter smog episodes [19]. The city has been at the center of legal disputes over diesel bans and has introduced environmental zones, public transport incentives, and improved cycling infrastructure in response [20].

The COVID-19 pandemic-induced lockdowns provided a unique opportunity to observe the effects of abrupt anthropogenic emission reductions [21]. Across Europe, studies reported 20–50% declines in NO_2 due to reduced traffic [22] and 0–30% reductions in PM2.5, while O_3 concentrations frequently increased due to altered photochemical chemistry [23]. Analysis by the German Environmental Agency (UBA) confirmed sharp declines in traffic-related NO_2 but noted that PM2.5 levels remained elevated in some regions due to increased residential heating and agricultural emissions [16]. These findings highlight the need for multi-sectoral pollution control strategies beyond traffic-focused restrictions [24].

Previous studies in Stuttgart primarily relied on city-wide or background monitoring stations. Data from official monitoring networks (e.g., Landesanstalt für Umwelt Baden-Württemberg (LUBW)) often reflect averaged urban conditions [25], thereby overlooking hyperlocal variations in high-traffic microenvironments like Marienplatz, Stuttgart's busiest pedestrian-traffic intersection. Existing work emphasized NO_2 and PM2.5 reductions during strict lockdown periods (March–May 2020), confirming 30–50% declines in NO_2 but

showing limited reductions in PM2.5 due to residential heating [24]. Few studies analyzed NO (nitrogen monoxide), CO (carbon monoxide; a key traffic proxy), or O_3, despite their importance in understanding traffic patterns and atmospheric photochemistry. Furthermore, earlier assessments did not evaluate the long-term post-lockdown rebound (2021–2022), leaving unanswered questions about whether pollutant levels returned to pre-pandemic baselines [22] or not. Likewise, there has been limited assessment of sustained behavioural changes, for example, on remote work, and their implications for post-pandemic air quality. Previous studies also largely neglected meteorology-pollution interactions, despite Stuttgart's basin topography exacerbating pollution accumulation and complicating the interpretation of meteorologically driven versus emission-driven changes effects [19].

To address these gaps, this study aims to: (a) quantify impacts of COVID-19 lockdowns on air pollutant concentrations (NO_2, NO, O_3, CO, PM2.5, PM10) at Marienplatz, a previously unstudied urban hotspot, by comparing the pre-lockdown (2018–2019), lockdown (2020), and post-lockdown (2021–2022) phases and assessing whether pollutant concentrations rebounded or stabilized; (b) decouple meteorological influences from emission-driven trends by modelling adjusted pollutant behaviour (e.g., PM2.5—humidity and O_3—temperature relationships) and evaluating weekly activity patterns to isolate traffic-linked effects, and (c) analyse pollutant interactions through NO/NO_2 ratios to distinguish traffic-related versus background contributions and assess O_3–NO_x—temperature dependencies.

Although numerous studies have documented short-term improvements in air quality during COVID-19 lockdowns, several important questions remain unresolved. In particular, distinguishing emission-driven changes from meteorologically driven variability remains a major challenge in urban air-quality assessment. Additionally, relatively few studies have combined explainable machine-learning approaches with directional source diagnostics to evaluate both the drivers and spatial origins of urban air pollution in the post-lockdown period. This study addresses these gaps by integrating meteorological normalization, SHAP-based feature attribution, and directional source analysis using a long-term dataset (2018–2022) from Stuttgart, a city characterized by complex basin topography and strong meteorological controls on pollutant dispersion.

This study presents the first comprehensive analysis of COVID-19 lockdown impacts on air quality at Stuttgart's Marienplatz, utilizing unique high-resolution, long-term (2018–2022) monitoring data. By integrating multi-pollutant measurements (NO_2, NO, O_3, CO, PM2.5, PM10) with meteorological parameters at this critical traffic hotspot, we: (1) quantify hyperlocal pollution trends and distinguish meteorological influences from emission-related changes using machine-learning-based meteorological normalization and chemical-regime shift analysis, (2) conduct wind-sector-resolved source apportionment of air pollutants to evaluate the persistence of post-lockdown air-quality improvements and identify directional emission dependencies, and (3) examine non-linear relationships between humidity metrics and particulate matter under reduced primary emissions, with implications for secondary aerosol formation in urban basins. Collectively, these analyses advance the understanding of urban microenvironment response to emission reductions and provide actionable insights for targeted air-quality management strategies in complex urban settings.

2. Materials and Methods

2.1. Study Area and Pollutant Monitoring Stations

Stuttgart is the capital and largest city of the German state of Baden-Württemberg [26]. It is located along the Neckar River within a verdant valley known as the "Stuttgart Cauldron," approximately one hour from both the Swabian Jura and the Black Forest. The city has a population of around 636,000, making it the sixth biggest city in Germany [27].

The surrounding administrative region hosts approximately 2.8 million inhabitants, while the wider metropolitan region comprises about 5.3 million people, ranking it among Germany's largest metropolitan regions [28].

Stuttgart's complex topography necessitates multiple monitoring stations in various locations to capture air quality variations and pollutant concentration levels. Marienplatz, located along the path of cold air currents descending from Nesenbach towards central Stuttgart, is a strategic site for monitoring pollutant deposition. This justified the installation of a stationary monitoring station that continously measures NO, NO_2, NO_x (oxides of nitrogen), O_3, CO, PM2.5, PM10, and BC (black carbon). The station is also equipped with meteorological sensors recording relative humidity, precipitation, air temperature, wind speed, and wind direction, providing valuable insights into both the pollution origins and atmospheric processes influencing pollutant dirspersion [29].

Marienplatz, situated in Stuttgart-Süd (Figure 1 (left)), functions as a central urban centre and major transit intersection. Its geographical coordinates, approximately 48.7656° N latitude and 9.1670° E longitude, situate it within a valley basin that strongly influences local air quality dynamics. Cold air current from Kaltental shapes pollutant distribution patterns, while dense surrounding development limits ventilation and contributes to an urban heat island effect [30]. Daily population density at Marienplatz nearly doubles due to commercial and commuter activity, except during the COVID-19 lockdowns when such activities were significantly reduced.

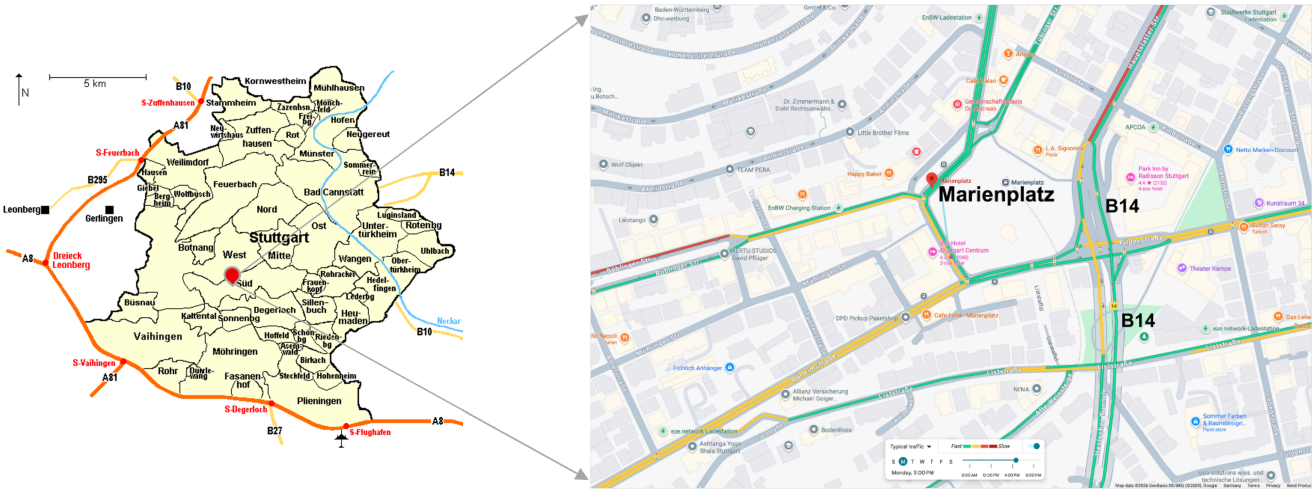

Figure 1. Map showing the location of Marienplatz and its traffic view.

Figure 1 (right) depicts the traffic configuration surrounding Marienplatz, which is bordered by three major roads: Filderstraße to the south, Marienplatz to the west and northwest, and Hauptstätter Straße (B14) to the east, each serving as a substantial emission sources. This location was chosen for this research since it is one of Stuttgart's pollution hotspots with elevated human exposure.

Since 1980, the State Institute of Baden-Württemberg (LUBW) has operated an air-quality measurement network across the region, while the City of Stuttgart's Office for Environmental Protection has conducted additional monitoring at various stations since 1965 [31]. LUBW provides comprehensive, up-to-date air-pollution data that reflect the human health exposure to various air pollutants [32]. Continuous air-quality monitoring at Marienplatz began in 2017 under the "Urban Climate Under Change" research initiative financed by the German Federal Ministry of Education and Research (BMBF) [33].

2.2. Data Collection Period

Accurate definition of the study period is a critical methodological step in assessing the impact of COVID-19 lockdown measures on air quality. This determination is rooted in an understanding of the temporal progression of the pandemic, including the epidemiological trends and the government interventions in Stuttgart City. The lockdown phases considered in this study are categorized into three distinct periods based on government-imposed restrictions and mobility limitations:

HL-1 (hard lockdown): 22 March 2020 to 4 May 2020 (44 days),

PL-1 (partial lockdown): 2 November 2020 to 22 November 2020 (21 days), and

HL-2 (extended hard lockdown): 15 December 2020 to 26 February 2021 (74 days).

These phases reflect escalating government responses, including curfews, mask requirements, reductions in public-transport capacity, school closures, and the suspension of non-essential services. Table 1 summarizes the lockdown categories, associated COVID-19 severity, and implemented measures.

Table 1. COVID-19 Lockdowns in Stuttgart (Baden-Württemberg), Germany.

Date	Rank	Severity of COVID-19 Spread	Measures
22 March 2020 to 4 May 2020	Hard Lockdown (HL-1)	Multiple cases detected and deaths reported	Curfews were imposed in six German states (including Baden-Württemberg) while other states prohibited physical contact with more than one person from outside one's household.
2 November 2020 to 22 November 2020	Partial Lockdown (PL-1)	Second wave of the pandemic. The total number of reported infections since the start of the pandemic crossed one million on 27 November.	Physical distancing rules were tightened while schools and kindergartens remained open, but only temporarily halted the rise in case numbers.
15 December 2020 to 26 February 2021	Hard Lockdown (HL-2)	The appearance of the Alpha variant and other mutations. Death rates in nursing homes remained high until late January 19, but dropped strongly in February, which was considered to be likely the result of residents and workers at these facilities having been prioritized in the vaccination campaign.	Made FFP2 masks or other clinical masks mandatory on public transport and in shops. Closing of some metro stations and an increase in public bus frequency service operating at <50% of capacity. Suspension of local and federal government services. Ceasing of operations at all non-essential industries

To establish a robust baseline, reference periods were selected from the corresponding calendar days in 2018, prior to any pandemic-related interventions. These baseline intervals serve as a control dataset, allowing for a comparative analysis of air quality under normal conditions versus that attributable to lockdown-induced emission reductions.

2.3. Measurement Devices, Data Sources, Availability, and SHAP Analysis

Between 2017 and 2022, the number of air quality monitoring stations in Stuttgart varied as the LUBW adapted its network to evolving environmental concerns. The network expanded in 2015 with the addition of five new NO_2 monitoring sites and a new station along Hauptstätter Straße measuring NO_2 and PM10. Further upgrades occurred in 2019.

For this study, air quality and meteorological datasets (2018–2022) were obtained from Marienplatz station operated by the University of Stuttgart's Institute of Combustion and Power Plant Technology (IFK). Air pollutant time series were analyzed using daily averages to capture high-frequency variability and monthly averages to characterize seasonal and

long-term trends. All pollutant concentrations were normalized; linear scaling was applied to all y-axes except CO, which employed a logarithmic scale due to its wider dynamic range.

Data completeness varied by pollutants and years because of instrument maintenance and temporary station operational interruptions. In particular, PM2.5 and PM10 measurements in 2022 exhibited reduced data coverage (25.9%). Consequently, trend interpretation for particulate matter was performed with caution and was based primarily on the multi-year behaviour of meteorologically normalized trends rather than reliance on single-year datasets. Figure 2 summarizes pollutant-specific completeness. Daily average concentrations were calculated only when ≥18 h of valid data were available; no imputation was performed. Lockdown—phase pollutant concentrations (HL-1, PL-1, HL-2; 2020–2021) were compared with baseline periods using non-parametric tests (Mann–Whitney U) and bootstrap confidence intervals, with seasonal adjustment to account for natural variability. Results with <60% completeness are flagged due to the increased uncertainty. Instrumentation specifications are provided in Tables A1 and A2.

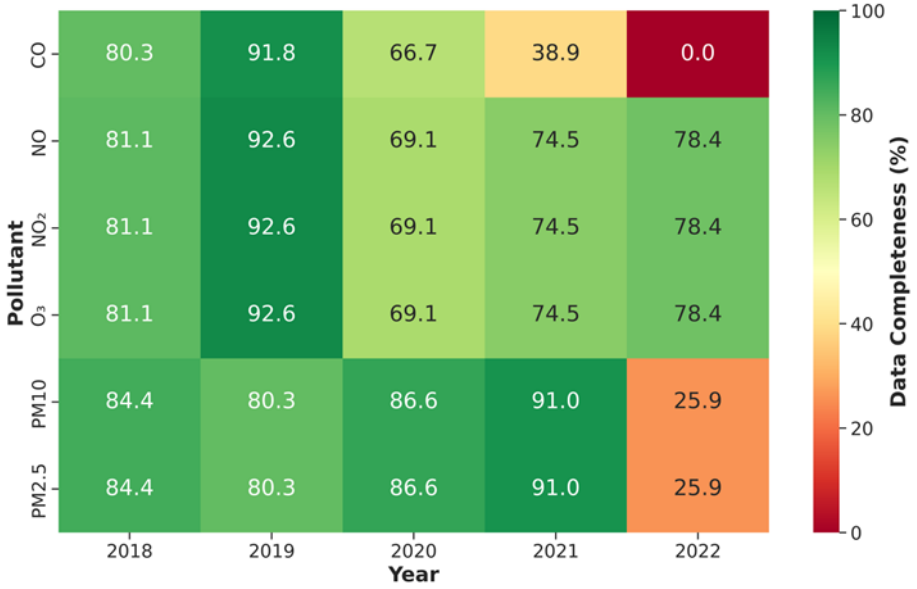

Figure 2. Data Completeness by Pollutant and Year.

To assess the relative influence of meteorological variables on pollutant concentrations, SHAP (SHapley Additive exPlanations) analysis was applied to the trained machine-learning models. SHAP is an explainable artificial intelligence method derived from cooperative game theory that quantifies the contribution of each input variable to individual model predictions through the calculation of Shapley values. In this framework, each predictor variable (e.g., temperature, wind speed, radiation, humidity) is treated as a "player" contributing to the final prediction, allowing the relative importance and direction of influence of meteorological factors to be evaluated. It should be noted that SHAP values describe how the model uses the input variables to generate predictions, indicating statistical influence rather than direct causal effects. This approach enables a transparent evaluation of the relative importance and direction of meteorological drivers in shaping pollutant concentrations.

3. Results and Discussion

A key consideration in interpreting these results is the incomplete data record for several pollutants (Figure 2). Data coverage was particularly limited for PM2.5 and PM10 in 2022 (25.9% completeness) and for CO in 2021 (38.9% completeness), with no CO measurements available for 2022. Consequently, analyses involving these pollutants should

be interpreted with caution, especially when assessing long-term trends. In this study, trend estimates for PM2.5 and PM10, and CO are therefore treated as indicative rather than definitive and are discussed primarily to highlight potential patterns rather than statistically robust long-term changes. By contrast, NO, NO_2, and O_3 datasets exceeded 60% completeness, providing greater confidence in the interpretation of their temporal trends.

3.1. Temporal Trends of Air Pollutants (2018–2022) at Marienplatz, Stuttgart

Figure 3 illustrates the annual evolution of key air pollutant concentrations at Marienplatz, Stuttgart, from 2018 to 2022, contextualized by the timing of three COVID-19 lockdown phases. The pandemic and associated restrictions represent a unique natural experiment, offering valuable insight into the relationship between human activity, emissions, and air quality. Over these five years, the observed data reveal divergent trends among pollutants.

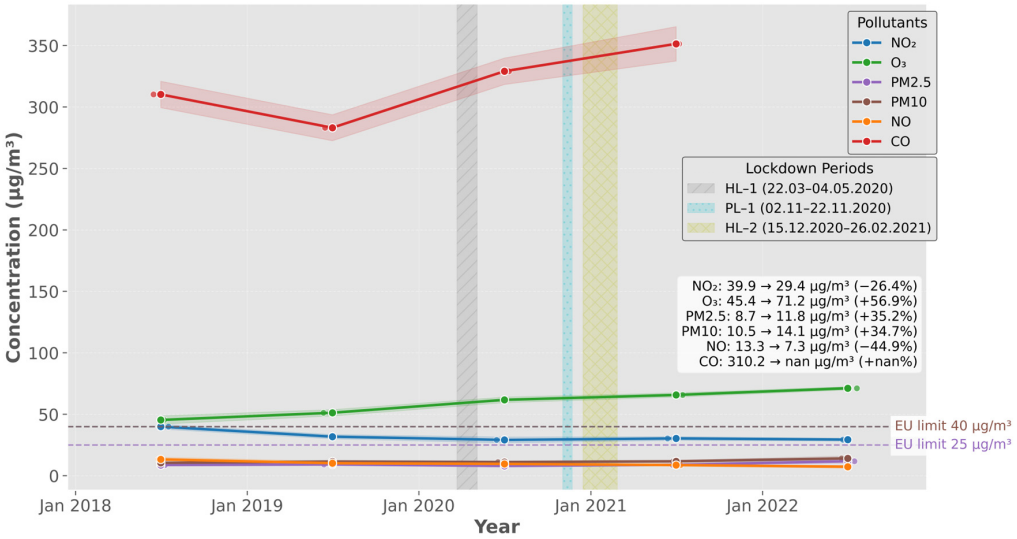

Figure 3. Air pollutant concentrations, including lockdown periods at Marienplatz, Stuttgart.

Carbon monoxide (CO) exhibited a non-intuitive trend. The concentration curve indicates an initial decrease from 2018 to 2019. However, this trend reversed, and CO levels began a steady increase from 2019 that persisted throughout the subsequent lockdown periods (2020–2021). While the CO raw data for year 2022 is not available, this sustained rise during a time of reduced mobility suggests that the dominant source of CO at this location was likely not vehicular traffic, but rather other combustion sources such as residential heating, which may have increased as people spent more time at home [14,34].

Concentrations of nitrogen dioxide (NO_2) and nitrogen oxide (NO) showed substantial declines by 26.4% (from 39.9 to 29.4 µg/m^3) and 44.9% (from 13.3 to 7.3 µg/m^3), respectively. These reductions reinforce the impact of reduced vehicular traffic and combustion sources during and after the lockdown periods [14,35]. The temporal alignment of the lockdown phases, particularly HL-1, with the most pronounced drops highlights the immediate effect of curtailed activity. Post-lockdown concentrations stabilized below pre-pandemic levels, suggesting some persistence of reduced emissions [14,36].

In contrast, ozone (O_3) concentrations increased significantly by 56.9%, rising from 45.4 µg/m^3 in 2018 to 71.2 µg/m^3 in 2022. This rise is consistent with the expected photochemical response to lower NO_x levels, as reduced titration allows for greater ambient ozone accumulation [23,37]. The increase in O_3 underscores the complex interplay between precursor emissions and atmospheric chemistry.

Apparent increases in PM2.5 and PM10 were observed over the study period, with PM2.5 rising from 8.7 to 11.8 μg/m^3 and PM10 from 10.5 to 14.1 μg/m^3. However, these apparent increases must be interpreted cautiously because data coverage for PM was substantially lower in 2022 (around 25.9%). As a result, the calculated percentage changes should not be interpreted as robust long-term trends but rather as indicative patterns within a partially incomplete dataset. Potential contributing factors may include residential heating, wood combustion, secondary aerosol formation, and regional transport [14,34], but confirming these influences would require more complete multi-year measurements. The steady rise in particulate matter concentrations highlights the need to address a broader range of emission sources beyond traffic [38].

Figure 4, with a multi-panel, illustrates the daily and 30-day mean concentrations of NO_2, NO, O_3, CO, PM2.5, PM10, and Figure 5 illustrates the yearly distributions of the key air pollutants at Marienplatz, Stuttgart, over five years. The background shading of Figure 4 denotes three distinct periods: pre-lockdown (2018–2019, light blue), lockdown (2020, light pink), and post-lockdown (2021–2022, light green). The lockdown period is further subdivided into hard and partial lockdowns.

The study period was segmented into pre-lockdown (2018–2019), lockdown (2020), and post-lockdown (2021–2022) intervals. Specific COVID-19 policy phases, Hard Lockdown 1 (HL-1: March–May 2020), Partial Lockdown (PL-1: November 2020), and Hard Lockdown 2 (HL-2: December 2020–February 2021), were annotated on the time series plots [14,39]. In the visualization, these phases are highlighted using background colour bands: dark red for HL-1, orange for PL-1, and dark red again for HL-2, allowing clear identification of the different restriction periods within the overall study timeline.

Both NO_2 and NO exhibited pronounced decreases during the 2020 lockdown, with the lowest concentrations observed during the hard lockdown phases, consistent with significant reductions in vehicular traffic and combustion-related activities [35,36]. Levels partially rebounded post-lockdown but remained below pre-pandemic values, indicating some persistent reduction in emissions [14].

O_3 displayed an inverse trend, surging during HL-1 and peaking at 47.8 μg/m^3, a classic photochemical response to reduced NO emissions and diminished ozone titration [23,37]. Elevated O_3 levels persisted into the post-lockdown period, albeit with seasonal variation.

CO concentrations increased during the lockdown, reaching pronounced winter peaks of 310.2 μg/m^3 during PL-1 and 398.1 μg/m^3 during HL-2. These peaks are attributed to increased residential heating or localized combustion activities. However, because CO data coverage was limited in 2021 and unavailable in 2022, attributing this pattern to specific behavioral or energy-use changes is not possible within the scope of the available dataset [14,34]. A partial decline in mid-2021 reflected reduced traffic and meteorological influences [38].

Particulate matter trends further illustrate the complexity of urban air quality responses. PM2.5 showed a moderate decrease during the lockdown, while PM10 exhibited only minor changes, spiking to 20.7 μg/m^3 during HL-1, likely due to dust resuspension and residential burning [14,34]. The limited reduction in PM10 suggests that sources such as regional transport, resuspension, and non-traffic emissions play a significant role [38].

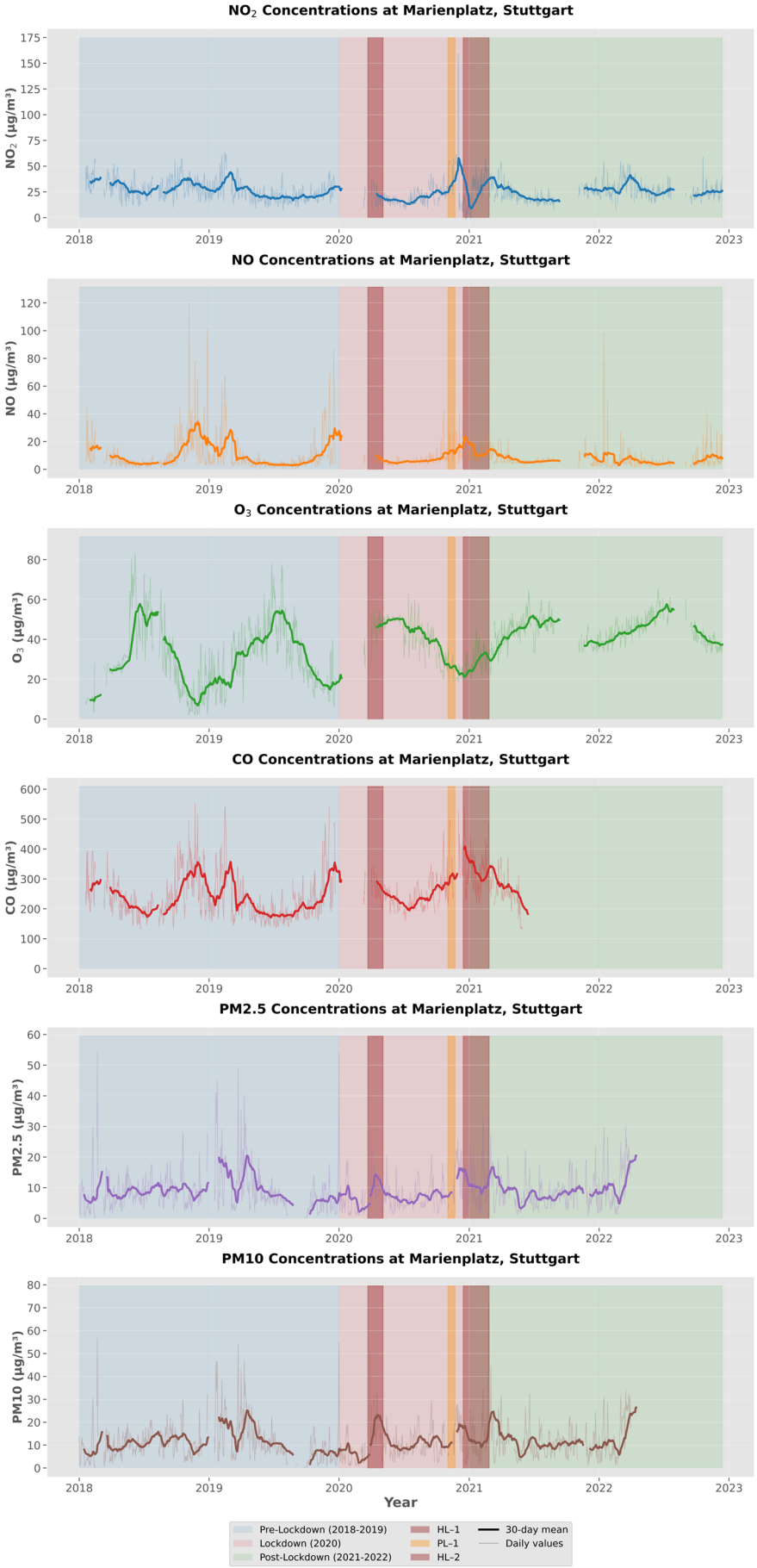

Figure 4. Time series comparison of pollutant concentrations at Marienplatz, Stuttgart, from 2018 to 2022.

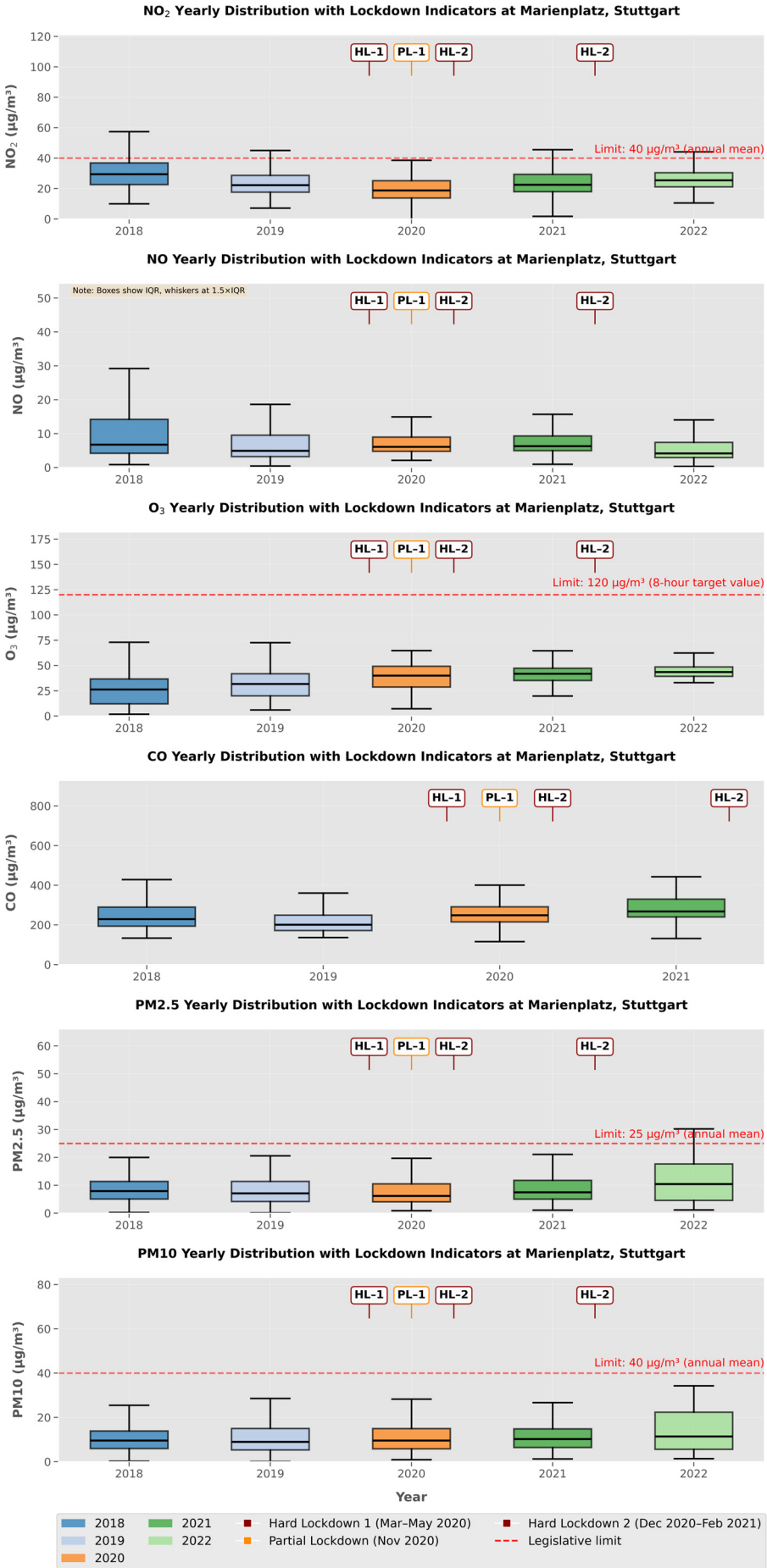

Figure 5. Annual distributions of key air pollutants (2018–2022) at Marienplatz, Stuttgart.

Collectively, these results demonstrate immediate air quality improvements during the COVID-19 lockdown, especially for traffic-related pollutants (NO_2, NO, and PM2.5). The persistent, though attenuated, post-lockdown reductions may indicate lasting behavioral or policy changes such as increased remote work [36]. The observed increase in ozone underscores the complexity of urban atmospheric chemistry, where reductions in primary emissions can have counterintuitive effects on secondary pollutants [23,37]. These findings highlight both the immediate and lasting impacts of lockdowns on urban air quality, as well as the influence of seasonal and source-specific factors [14].

The quantitative assessment at Marienplatz, Stuttgart (Table 2), shows clear pollutant-specific responses to lockdown measures. Nitrogen dioxide declined sharply, with median NO_2 concentration falling 22.5% during 2020 relative to the 2018–2019 baseline (from 31.5 to 24.4 $\mu g/m^3$). It partially rebounded post-lockdown, yielding a long-term reduction of −14.2%. Conversely, NO showed a slight increase of 5.5% during lockdown (from 6.2 to 6.5 $\mu g/m^3$), with a modest long-term decrease of −2.3%. O_3 increased 43.1% during the lockdown (from 44.7 to 64.0 $\mu g/m^3$) and remained elevated post-lockdown, resulting in a long-term increase of +52.9%. CO levels rose 15.7% from 268.9 to 311.0 $\mu g/m^3$ in 2020; post-lockdown data were insufficient for trend calculation. Particulate matter changes were mixed: PM2.5 fell during lockdown (from 7.5 to 6.2 $\mu g/m^3$) but showed a slight long-term increase of +1.8%. PM10 remained nearly stable during lockdown (+0.9%) but increased post-lockdown, resulting in a long-term rise of +9.1%.

Table 2. Quantitative assessment of lockdown impacts at Marienplatz, Stuttgart.

Pollutant	Pre-Lockdown 2018–2019 Median ($\mu g/m^3$)	Lockdown 2020 Median ($\mu g/m^3$)	Post-Lockdown 2021–2022 Median ($\mu g/m^3$)	Lockdown Reduction (%)	Long-Term Trend (%)
NO_2	31.5	24.4	27.0	−22.5	−14.2
NO	6.2	6.5	6.0	+5.5	−2.3
O_3	44.7	64.0	68.4	+43.1	+52.9
CO	268.9	311.0	Insufficient dataset	+15.7	-
PM2.5	7.5	6.2	7.7	−17.8	+1.8
PM10	9.5	9.6	10.3	+0.9	+9.1

Figure 6 (violin plots) compares weekday and weekend pollutant concentrations for NO_2, NO, O_3, CO, PM2.5, and PM10 at Marienplatz, Stuttgart, across three periods: pre-lockdown (2018–2019), lockdown (2020), and post-lockdown (2021–2022). The results reveal clear differences in the weekday-weekend dynamics for primary pollutants, especially during the pre-lockdown phase, and show how these patterns were altered by COVID-19 restrictions.

NO_2 and NO both exhibit significantly higher concentrations on weekdays than weekends in all periods, with the largest differences observed pre-lockdown (NO_2: $p < 0.0001$; NO: $p < 0.0001$). During the lockdown, this weekday-weekend gap narrows but remains statistically significant (NO_2: $p = 0.0021$; NO: $p = 0.0002$), reflecting the reduction in weekday traffic and economic activity. In the post-lockdown period, the difference persists (NO_2: $p = 0.0003$; NO: $p < 0.0001$), though the overall levels remain lower than pre-pandemic values. This pattern confirms that traffic-related emissions dominate NO_x levels and that mobility restrictions during lockdowns effectively reduced both the concentrations and the weekday-weekend contrast [14].

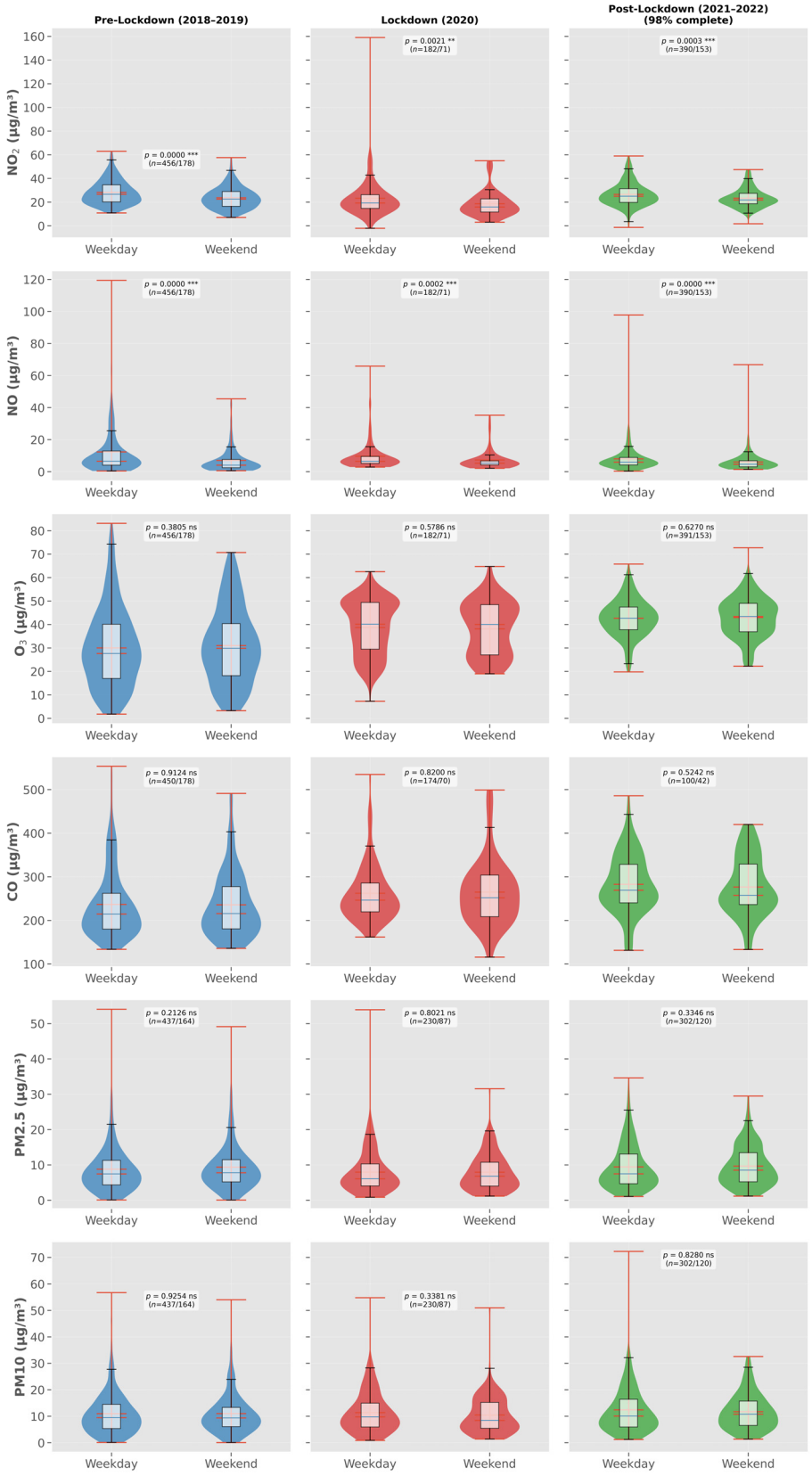

Figure 6. Comparison of weekday and weekend pollutant concentrations by period at Marienplatz, Stuttgart.

Ozone (O_3), in contrast, shows no significant difference between weekdays and weekends in any period (all p-values > 0.3), and its distributions remain relatively stable. This lack of a weekly cycle is consistent with the photochemical nature of ozone, which depends on precursor availability and meteorology rather than direct emissions [23,37]. Notably, median O_3 values are slightly higher during the lockdown, consistent with reduced NO titration when NO_x emissions are suppressed [37].

CO, PM2.5, and PM10 also display no significant weekday-weekend differences in any period (all p-values > 0.2), and their distributions are relatively broad but stable. This suggests that, at this site, these pollutants are less sensitive to short-term changes in local traffic patterns and are likely influenced by a mix of regional sources, secondary formation, and background concentrations [34,38].

Overall, the plots demonstrate that the COVID-19 lockdown substantially reduced both the absolute concentrations and the weekday-weekend contrasts for traffic-related pollutants (NO_2 and NO), while secondary and regionally influenced pollutants (O_3, CO, PM2.5, PM10) showed little change in their weekly cycles. These findings underscore the effectiveness of mobility restrictions for reducing urban NO_x pollution, but also highlight the resilience of ozone and particulate matter to short-term local interventions, pointing to the need for broader, multi-faceted air quality management strategies [14,37].

3.2. Quantification of Ozone Enhancement: Contribution of Reduced NO Titration and Photochemical Production

Figure 7 presents a quantitative assessment of the mechanisms responsible for the observed ozone (O_3) enhancement during the lockdown period by separating the relative contributions of reduced nitrogen oxide (NO_x) titration and enhanced photochemical production. As shown in Figure 7a, the mean O_3 concentration increased significantly by 13.2 ± 3.0 μg/m^3, while NO concentrations decreased by -2.0 ± 1.6 μg/m^3 during the lockdown period. The reduction in NO levels reflects decreased emissions from traffic and other combustion-related sources following mobility restrictions and reduced anthropogenic activities. Similar declines in NO_x emissions during COVID-19 lockdown periods have been widely reported in urban environments globally [21,23,40].

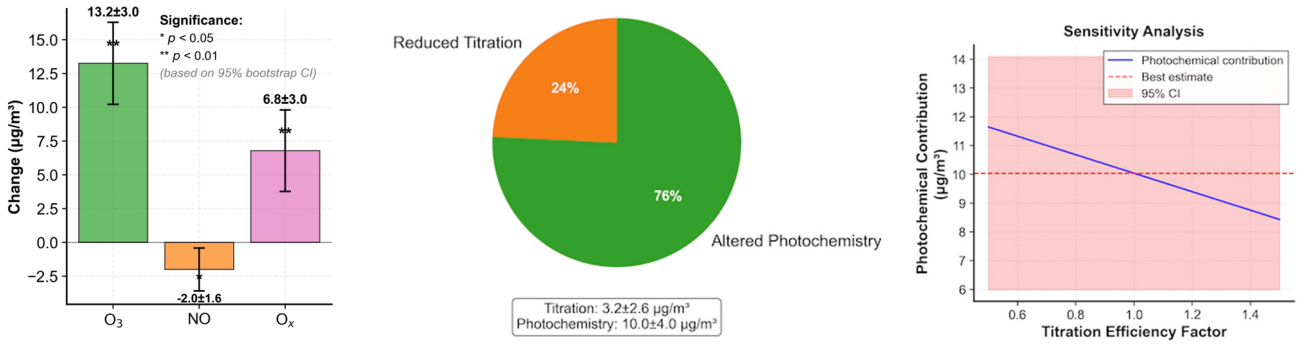

Figure 7. Quantification of the mechanisms driving ozone (O_3) enhancement during the lockdown period. (**a**) Mean concentration changes in O_3, NO, and total oxidant (O_x = O_3 + NO_2) between the pre-lockdown and lockdown periods. (**b**) Decomposition of the total observed ozone increase (ΔO_3 = 13.2 μg/m^3) into contributions from reduced NO titration (24%) and enhanced photochemical production (76%). (**c**) Sensitivity analysis showing the estimated photochemical contribution to ΔO_3 under different assumptions of titration efficiency.

In addition, total oxidant (O_x = O_3 + NO_2) increased by 6.8 ± 3.0 μg/m^3, indicating that the observed ozone increase cannot be attributed solely to reduced NO titration. Since O_x is often considered a conserved indicator of the photochemical oxidant budget, its

increase suggests that enhanced net photochemical ozone formation occurred during the lockdown period [41,42]. These findings highlight the importance of considering both emission reductions and atmospheric chemical processes when interpreting changes in urban ozone concentrations.

The relative contributions of the two mechanisms are illustrated in Figure 7b. The total ozone increase (ΔO_3 = 13.2 $\mu g/m^3$) is decomposed into reduced titration (24%) and enhanced photochemical production (76%). The reduced titration component (3.2 ± 2.6 $\mu g/m^3$) arises from lower NO concentrations limiting the ozone destruction reaction NO + O_3 → NO_2 + O_2 [42]. In contrast, the dominant contribution (10.0 ± 4.0 $\mu g/m^3$) is attributed to enhanced photochemical production, suggesting that the reduction in NO_x emissions altered the atmospheric chemical regime in a way that favored ozone formation. This interpretation is supported by the increase in the O_3/NO_2 ratio from 1.50 during the pre-lockdown period to 2.70 during the lockdown, indicating a shift toward a more oxidizing atmospheric environment. Concurrent decreases in NO_2 (−6.5 ± 2.7 $\mu g/m^3$) and NO (−8.5 $\mu g/m^3$) further confirm the substantial reduction in NO_x emissions. Such nonlinear ozone responses to NO_x reductions are characteristic of VOC-limited or transitional photochemical regimes, commonly observed in urban environments [23,41,43].

Figure 7c presents a sensitivity analysis assessing the robustness of the estimated photochemical contribution under varying assumptions of titration efficiency, which represents the effectiveness of NO in removing ozone via chemical titration. As the titration efficiency factor increases from 0.5 to 1.5, the estimated photochemical contribution decreases from approximately 11.7 $\mu g/m^3$ to 8.4 $\mu g/m^3$, illustrating the trade-off between suppressed ozone destruction and enhanced photochemical production. Despite this variability, the best estimate of approximately 10 $\mu g/m^3$ remains within the 95% confidence interval (6–14 $\mu g/m^3$) across the tested range, indicating that the dominance of photochemical production is robust to uncertainties in the titration parameterization. These results are consistent with previous studies demonstrating that reductions in NO_x emissions can lead to complex and sometimes counterintuitive ozone responses depending on the prevailing photochemical regime and precursor availability [40,42,43]. Overall, the analysis indicates that although reduced NO titration contributed to the observed ozone enhancement during the lockdown period, enhanced photochemical production was the primary driver of the increase in O_3 concentrations.

3.3. Photochemical Regime Analysis and Transition During the Lockdown Period

Figure 8 presents a comprehensive analysis of the photochemical ozone formation regime using the O_3/NO_2 ratio, NO/NO_2 ratios, and total oxidant (O_x = O_3 + NO_2) production efficiency. The distribution of the O_3/NO_2 ratio (Figure 8a) provides a diagnostic indicator of the dominant ozone formation regime. The median O_3/NO_2 ratio increased from 1.50 during the pre-lockdown period (2018–2019) to 2.70 during the lockdown period (2020) and remained relatively high at 2.46 during the post-lockdown period (2021–2022). According to established photochemical regime thresholds, values above approximately 2 typically indicate NO_x-limited conditions, whereas lower ratios correspond to NO_x-saturated (VOC-limited) regimes [41,43]. The observed increase in the O_3/NO_2 ratio during the lockdown, therefore, suggests a shift toward stronger NO_x-limited photochemistry, likely driven by the substantial reduction in traffic-related NO_x emissions.

The temporal evolution of the 30-day rolling O_3/NO_2 ratio (Figure 8b) further illustrates the transition between photochemical regimes across the study period. Prior to the lockdown, the ratio frequently fluctuated between NO_x-saturated and transitional regimes, reflecting the influence of strong local NO_x emissions typical of urban environments. However, during the lockdown periods (HL-1, PL-1, and HL-2), the ratio consistently exceeded

the NO_x-limited threshold, indicating that reduced NO_x emissions shifted the chemical environment toward conditions more favorable for net ozone production. Similar transitions in photochemical regimes during COVID-19 lockdowns have been reported in several urban regions worldwide, where reduced NO_x emissions altered the balance between ozone production and destruction processes [21,23,40].

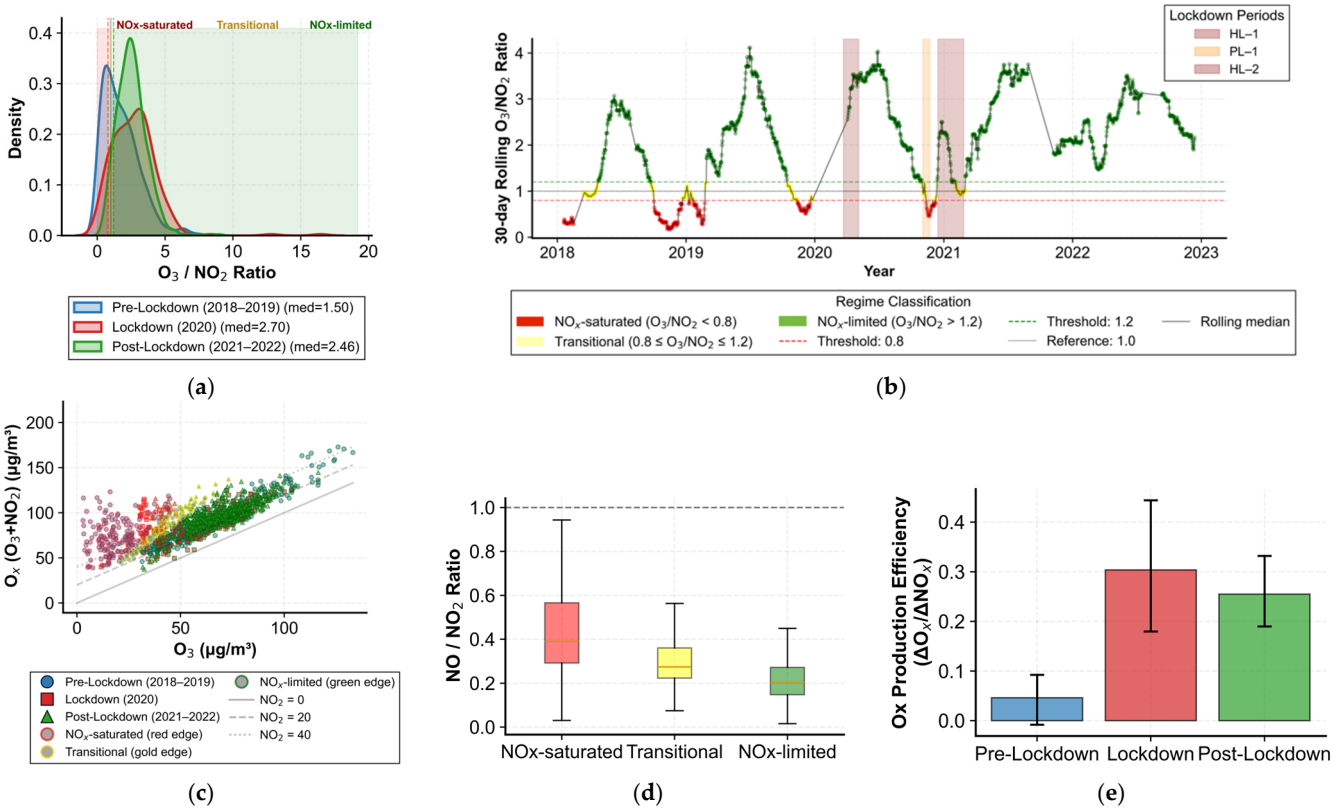

Figure 8. Photochemical regime analysis and transition detection during the study period (2018–2022). (**a**) Kernel density distribution of the O_3/NO_2 ratio for the pre-lockdown (2018–2019), lockdown (2020), and post-lockdown (2021–2022) periods. (**b**) Temporal evolution of the 30-day rolling O_3/NO_2 ratio from 2018 to 2022. (**c**) Relationship between total oxidant ($O_x = O_3 + NO_3$) and O_3 concentrations under different periods, illustrating the consistency of oxidant production across photochemical regimes. (**d**) Boxplot distribution of the NO/NO_2 ratio for the three photochemical regimes (NO_x-saturated, transitional, and NO_x-limited). (**e**) O_x production efficiency ($\Delta O_x/\Delta NO_x$) for the pre-lockdown, lockdown, and post-lockdown periods, indicating the effectiveness of NO_x emission changes in producing photochemical oxidants.

The relationship between O_x and O_3 concentrations under different regimes (Figure 8c) provides additional insight into the underlying atmospheric chemistry. A strong positive correlation between O_3 and O_x is observed across all periods, indicating that increases in ozone are associated with enhanced regional oxidant production rather than solely reduced local titration by NO. The clustering of data points shows a shift toward higher O_x values during the lockdown and post-lockdown periods, suggesting enhanced photochemical oxidant formation despite reductions in primary pollutant emissions. This behavior is consistent with previous studies showing that decreases in NO_x emissions in NO_x-saturated environments can enhance net ozone production due to reduced titration and altered radical chemistry [42,43].

Further insights into the photochemical regime are provided by the NO/NO_2 ratio distribution (Figure 8d). The NO/NO_2 ratio decreases progressively from NO_x-saturated conditions to NO_x-limited regimes, reflecting reduced fresh NO emissions and increased photochemical oxidation of NO to NO_2. Median values decrease from approximately 0.39

in NO_x-saturated conditions to 0.20 under NO_x-limited conditions, indicating enhanced atmospheric oxidation capacity during periods with lower NO_x emissions. This pattern is consistent with the expected chemical behavior of urban atmospheres transitioning from emission-dominated to photochemically driven regimes [41,43].

The O_x production efficiency ($\Delta O_x/\Delta NO_x$) shown in Figure 8e further confirms the enhanced photochemical activity during the lockdown period. The production efficiency increased substantially from 0.046 in the pre-lockdown period to 0.304 during lockdown, before slightly decreasing to 0.255 in the post-lockdown period, while remaining significantly higher than pre-lockdown levels. Increased oxidant production efficiency indicates that each unit reduction in NO_x emissions resulted in a relatively larger increase in photochemically produced oxidants. Such behavior has been widely observed in urban environments where NO_x emission reductions move the system closer to NO_x-limited conditions, thereby increasing the efficiency of ozone formation [41,42].

Overall, the statistical summary presented in Table 3 confirms that the study region remained predominantly NO_x-limited throughout the study period, with the highest oxidant production efficiency occurring during the lockdown period. These results demonstrate that reductions in anthropogenic emissions significantly altered the atmospheric chemical regime, enhancing photochemical oxidant formation despite overall decreases in primary pollutants. The findings highlight the nonlinear response of urban ozone chemistry to emission reductions and underscore the importance of coordinated NO_x emission control strategies to effectively mitigate ozone pollution [41,43].

Table 3. Statistical summary by period.

Period	O_3/NO_2	Regime	NO/NO_2	O_x Eff	n
Pre-Lockdown	1.50	NO_x-limited	0.20	0.046	634
Lockdown	2.70	NO_x-limited	0.28	0.304	253
Post-Lockdown	2.46	NO_x-limited	0.23	0.255	543

3.4. Meteorologically Normalized Air Quality Trends in the Context of COVID-19 Lockdown Measures

It is important to recognize that raw pollutant concentrations are subject to significant meteorological variability, which can obscure or exaggerate underlying emission-driven trends [22,44]. The analysis of meteorologically normalized trends (Figure 9) for major air pollutants at Marienplatz, Stuttgart, from 2018 to 2022, provides a comprehensive view of the interplay between emission changes, meteorological variability, and policy interventions such as the COVID-19 lockdown.

The results for carbon monoxide (CO) show a pronounced and sustained decline over the study period, with raw concentrations frequently exceeding 300 $\mu g/m^3$ during 2018–2019. This high variability and magnitude sharply decreased during the 2020 lockdown and remained lower in the post-lockdown years [38,39]. The meteorologically normalized CO trend closely follows the central tendency of the raw data but effectively eliminates short-term weather-driven fluctuations, confirming that the observed long-term decline is primarily attributable to reductions in local emissions rather than meteorological effects [22,44]. The temperature context, with higher CO concentrations during colder months, underscores the role of seasonal heating and atmospheric dispersion, but the persistent downward trend in normalized CO concentrations points to structural emission changes as the dominant factor in improved air quality [34].

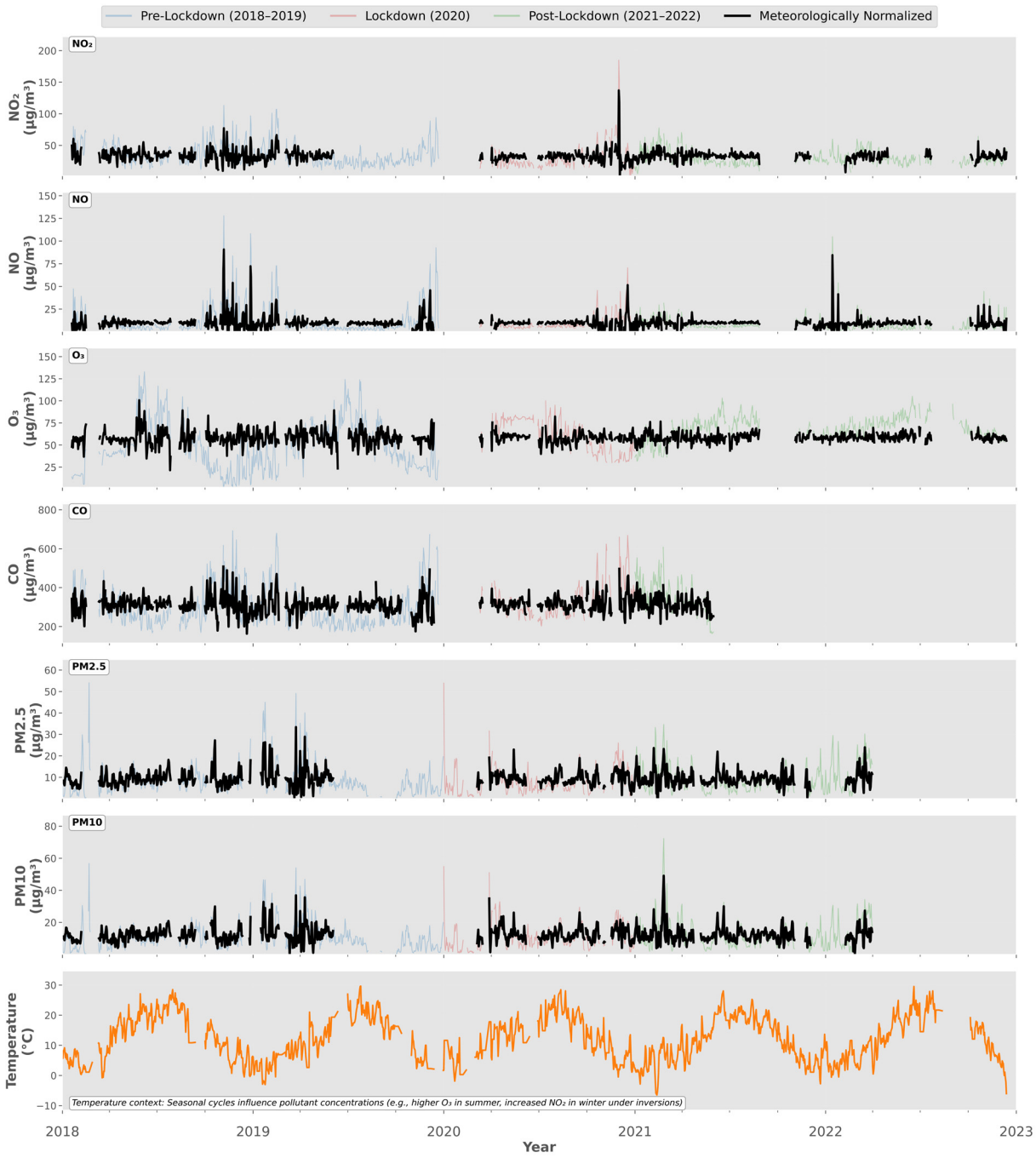

Figure 9. Meteorologically Normalized Air Quality Trends at Marienplatz, Stuttgart.

For nitrogen monoxide (NO), concentrations pre-lockdown were highly variable, with frequent peaks above 45 µg/m^3. The 2020 lockdown period saw a marked reduction in both the frequency and magnitude of these peaks, reflecting a significant drop in emissions likely due to decreased traffic and economic activity [35,37]. Post-lockdown, NO levels partially rebounded but remained below pre-lockdown values. The meteorologically normalized trend for NO reveals a distinct reduction during the lockdown, with only a modest increase afterward, suggesting that emission reductions had a lasting effect beyond meteorological influences. Nitrogen dioxide (NO_2) exhibited a similar pattern, with pre-lockdown concentrations typically between 30 and 50 µg/m^3, a sharp decrease during lockdown, and a persistent reduction post-lockdown. The normalized NO_2 trend closely

follows the original data, with reduced noise, supporting the conclusion that emission changes, not weather, drove the observed decreases [22,44].

Ozone (O_3) trends contrasted with those of NO and NO_2. Pre-lockdown, O_3 concentrations showed expected seasonal cycles, peaking in summer. During the lockdown, O_3 levels increased, particularly in the normalized trend, which highlights a clear rise in 2020. Post-lockdown, O_3 remained elevated compared to pre-lockdown levels, and the normalized trend indicates that this increase is not solely due to temperature or meteorological factors. This pattern is consistent with the inverse relationship between O_3 and NO_x, where reduced NO emissions diminish O_3 titration, leading to higher ambient ozone concentrations [23,37].

Particulate matter trends for PM10 and PM2.5 further reinforce the impact of emission reductions. Pre-lockdown PM10 levels were highly variable, with frequent peaks above 20 $\mu g/m^3$ and occasional spikes over 40 $\mu g/m^3$. The 2020 lockdown brought a visible reduction in both the frequency and magnitude of PM10 peaks, as confirmed by the normalized trend [34,38]. Post-lockdown, PM10 concentrations increased slightly but remained below pre-lockdown levels, with the normalized trend indicating persistent emission reductions or changes in source contributions. PM2.5 followed a similar trajectory, with pre-lockdown values often above 15 $\mu g/m^3$ and peaks over 35 $\mu g/m^3$. The lockdown period saw a marked reduction in both the frequency and intensity of PM2.5 peaks, and the normalized trend shows a distinct, lasting decline. After restrictions were lifted, PM2.5 concentrations rose modestly but did not return to pre-lockdown values, highlighting the sustained impact of emission reductions [22,37].

Temperature trends, characterized by regular seasonal cycles, provide essential context for interpreting pollutant variability, especially for O_3 and particulate matter [23,44]. However, the meteorologically normalized trends across all pollutants demonstrate that the most significant improvements in air quality during and after the lockdown are attributable to emission changes rather than favourable weather conditions [22,37]. These findings underscore the efficacy of emission control measures and behavioural changes, such as those implemented during the COVID-19 lockdown, in driving sustained reductions in urban air pollution. The results are in line with broader European trends and support the continued implementation of integrated air quality management strategies targeting combustion-related sources [14,39]. The application of meteorological normalization is critical for disentangling the effects of weather from emission changes, providing robust evidence that structural emission reductions were the dominant factor in the observed improvements in air quality at Marienplatz during this period [22,44].

In summary (Table A3), the integration of raw and meteorologically adjusted analyses, together with the unique natural experiment provided by the COVID-19 lockdowns, offers a comprehensive understanding of recent air quality trends at Marienplatz, Stuttgart. Table A3 presents both the raw observed annual mean concentrations and the meteorologically adjusted trends for key pollutants from 2018 to 2022. The raw trends reflect observed concentrations influenced by both emissions and weather, while the adjusted trends isolate the emission-driven changes, allowing a clearer interpretation of underlying trends. While primary pollutant reductions reflect successful emission control measures and the immediate impact of reduced human activity, the persistent increases in ozone and particulate matter, both in raw and adjusted data, highlight the need for next-generation air quality management strategies. These should encompass not only traffic-related emissions but also residential, industrial, and secondary pollutant sources, while accounting for the growing influence of meteorological and climatic factors [14,22,44]. Such a holistic approach is essential for achieving sustained improvements in urban air quality and public

health, particularly in the face of future disruptions or behavioural shifts akin to those experienced during the COVID-19 pandemic [36,39].

3.4.1. Influence of Meteorology on Gaseous Pollutants

Meteorological normalization analyses were conducted for carbon monoxide (CO), nitrogen oxide (NO), nitrogen dioxide (NO_2), ozone (O_3), and particulate matter fractions (PM2.5 and PM10) to separate the respective influences of meteorological conditions and emission sources on observed concentration variability (Figure 10). The coefficients of determination (R^2) for NO (0.12) and NO_2 (0.13) indicate that meteorological factors account for only a small fraction of the variability in these primary pollutants [22,44]. This suggests that concentrations of NO and NO_2 at Marienplatz are predominantly driven by local emission sources, chiefly vehicular traffic, rather than by meteorological dispersion or chemical transformation processes [35,44]. The tight clustering of data points along the 1:1 line further supports this conclusion, indicating stable emission patterns with minimal modulation by meteorological conditions.

In contrast, O_3 and CO exhibit higher R^2 values of 0.29 and 0.23, respectively, reflecting greater sensitivity to meteorological drivers such as temperature, solar radiation, and atmospheric mixing height. For CO, this dependence also includes contributions from localized emission sources and dispersion variability. The behavior of O_3 is consistent with its secondary nature, as O_3 formation is strongly influenced by photochemical processes and meteorological variability [23,37]. The increased scatter observed in the O_3 normalization plot highlights the complexity of ozone dynamics in urban environments.

These results underscore a clear distinction between primary and secondary pollutants. Primary traffic-related pollutants are dominated by direct emissions, whereas O_3 concentrations are strongly modulated by meteorological factors [22,23]. The low R^2 values for NO and NO_2 also suggest that the confined urban canyon configuration at Marienplatz limits dispersion, further reinforcing the influence of local sources [44].

Particulate matter exhibited exceptionally low R^2 values for PM2.5 (0.06) and PM10 (0.09), indicating that only 5–9% of the observed variability can be attributed to meteorological conditions [22,44]. Most day-to-day fluctuations are therefore driven by local emission sources such as road traffic, domestic heating, and construction activities [14,34]. The scatter plots display dense clustering along the 1:1 line, with minor deviations at higher concentrations, particularly for PM10. The slightly higher R^2 value for PM10 may reflect a marginal influence of meteorological factors through resuspension processes [44].

Overall, particulate matter concentrations at this urban traffic site are largely insensitive to meteorological variability and are primarily controlled by emission dynamics. Consequently, long-term PM2.5 and PM10 trends at Marienplatz can be interpreted as reliable indicators of changes in local emissions rather than fluctuations in meteorological conditions [22,34].

3.4.2. Implications for Urban Air Quality Management

The meteorological normalization results highlight the dominant influence of local emissions on air quality at Marienplatz, particularly for primary gaseous pollutants and particulate matter [14,44]. The minimal role of meteorology enhances the robustness of trend analyses and supports the use of these data as sensitive indicators of emission control effectiveness. Conversely, the moderate meteorological dependence of ozone underscores the need for integrated air quality management strategies that address both precursor emissions and weather-related variability [23,37].

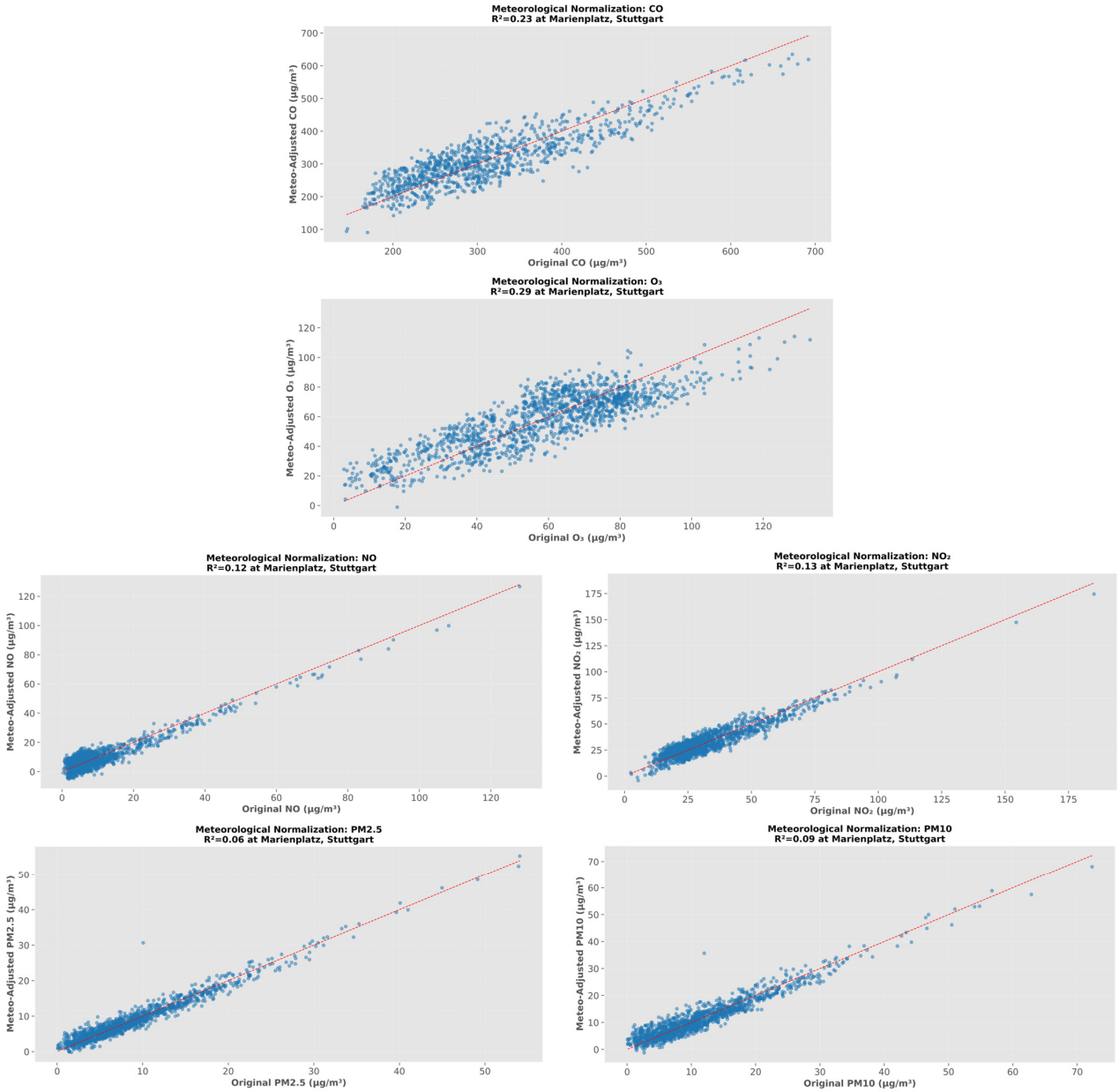

Figure 10. Meteorological normalization analysis for the pollutants concentration at Marienplatz, Stuttgart.

Overall, these findings indicate that meaningful improvements at traffic-dominated urban hotspots such as Marienplatz will require targeted emission reduction measures. However, because this study focuses on a single street-canyon monitoring site, the results primarily reflect localized emission dynamics and micro-scale dispersion conditions. Therefore, the conclusions should be interpreted as representative of high-traffic urban canyon environments rather than the entire city of Stuttgart. Dependence on favourable meteorological conditions alone is unlikely to produce substantial or lasting reductions in concentrations of primary pollutants or particulate matter [14,22]. The analyses also confirm that air quality at Marienplatz is predominantly controlled by localized emissions rather than meteorological variation. This validates the interpretation of observed pollutant trends as robust indicators of policy effectiveness and reinforces the need for sustained, emission-focused interventions to achieve lasting improvements in urban air quality [14,39].

3.4.3. Quantifying Meteorological Contributions to Pollutant Levels Using SHAP (Shapley Additive Explanations)

The SHAP framework decomposes the pollutant concentration prediction into additive contributions from each meteorological feature [45]. The SHAP bar plots (Figure A1) presented quantify the mean absolute SHAP values for key meteorological variables influencing the concentrations of CO, NO, NO_2, and O_3 at Marienplatz, Stuttgart. These plots provide a robust assessment of the relative importance of each meteorological factor within the predictive models for each pollutant [37,46].

For carbon monoxide (CO), temperature is the most influential meteorological variable, with a mean absolute SHAP value of +43.18, substantially exceeding those of the other variables. Humidity (+14.92), pressure (+10.53), and wind speed (+8.35) also contribute, though to a lesser extent. This indicates that temperature fluctuations exert the greatest impact on CO concentrations, likely due to their effects on emission rates and atmospheric mixing. Humidity and pressure further modulate CO levels, while lower wind speeds are associated with elevated concentrations as a result of reduced atmospheric dispersion [22,44].

In the case of nitrogen monoxide (NO), temperature again emerges as the dominant factor, with a mean absolute SHAP value of +3.96. Humidity (+1.50), pressure (+1.06), and wind speed (+0.92) play secondary roles. This pattern suggests that temperature-driven processes, including emission rates and chemical reactivity, are the primary determinants of NO variability. The lesser, but still notable, influence of humidity and pressure reflects their roles in atmospheric chemistry and stability, while the effect of wind speed underscores the importance of dispersion [35,44].

For nitrogen dioxide (NO_2), temperature remains the most significant meteorological driver (+5.42), followed by precipitation (+3.38), pressure (+2.21), humidity (+1.49), and wind speed (+1.17). The relatively high importance of precipitation highlights the effectiveness of wet scavenging in reducing NO_2 concentrations. The continued influence of pressure and humidity is consistent with their roles in atmospheric stability and secondary formation, while wind speed again reflects the importance of dispersion [22,44].

Ozone (O_3) displays a similar trend, with temperature as the leading driver (+9.69), followed by humidity (+4.19), wind speed (+2.70), pressure (+2.31), and solar radiation (+1.39). The strong impacts of temperature and radiation align with the photochemical nature of ozone formation, which is enhanced under warm and sunny conditions. Humidity and pressure also contribute, while the influence of wind speed underscores the importance of transport and mixing in modulating ozone levels [23,37].

Collectively, these SHAP bar plots consistently demonstrate that temperature is the most influential meteorological factor for all examined pollutants, particularly CO and O_3. Humidity, pressure, and wind speed also play important roles, with precipitation being especially significant for NO_2. These findings reinforce the central role of meteorological conditions in shaping urban air quality and highlight the necessity of accounting for weather variability in both air quality management and predictive modeling [22,44].

The SHAP bar plots for PM2.5 and PM10 at Marienplatz provide a clear, quantitative ranking of the meteorological variables most influential for these particulate pollutants. For PM2.5, temperature is the dominant variable (mean absolute SHAP value +1.91), suggesting that temperature fluctuations have the largest average impact on PM2.5 concentrations, likely due to their effects on atmospheric chemistry, secondary particle formation, and boundary layer dynamics. Precipitation (+1.15) and pressure (+1.06) are also significant contributors. The importance of precipitation underscores the role of wet scavenging in removing fine particles, while the influence of pressure reflects pollutant accumulation under stable, high-pressure conditions. Humidity (+0.56) and wind speed (+0.44) have

smaller but still notable impacts, with humidity potentially affecting secondary aerosol processes and wind speed influencing dispersion and dilution [22,44].

The PM10 plot reveals a more balanced influence among the top three variables: temperature (+1.73), precipitation (+1.83), and pressure (+1.62), all contribute substantially and nearly equally to PM10 variability. This indicates that, for coarser particulate matter, meteorological conditions related to atmospheric stability, precipitation events, and thermal dynamics are all critical. Humidity (+0.99) and wind speed (+0.66) also play important roles, with humidity potentially promoting particle growth and wind speed again facilitating pollutant dispersion [22,44].

Overall, these SHAP bar plots provide a global, model-agnostic measure of feature importance. The findings confirm that temperature, precipitation, and pressure are the dominant meteorological drivers for both PM2.5 and PM10 at this urban location, while humidity and wind speed have secondary but meaningful effects. This ranking is valuable for both scientific understanding and practical air quality management, as it identifies which meteorological factors should be prioritized in forecasting models and mitigation strategies. The results are consistent with the broader literature, which finds that particulate concentrations are highly sensitive to meteorological variability, especially in urban environments where local emissions and atmospheric processes interact dynamically [22,23,44].

3.4.4. SHAP Value Distributions for the Pollutants at Marienplatz, Stuttgart

The SHAP summary plot (Figure A2) analysis across all examined pollutants, NO, NO_2, O_3, PM2.5, CO, and PM10, provides a detailed understanding of how meteorological variables influence urban air quality at Marienplatz, Stuttgart. Temperature emerged as a universal positive driver for all pollutants, with particularly strong effects observed for NO, O_3, and CO. Elevated temperatures are likely to enhance emission rates from both anthropogenic and natural sources, stimulate photochemical reactions, and reduce atmospheric mixing heights, all of which contribute to increased pollutant concentrations [22,23,44]. This finding underscores the critical role of temperature in shaping the temporal variability and episodic peaks of urban air pollution, especially during heatwaves or summer months [47].

Precipitation was found to be a significant negative driver for NO_2, PM2.5, and PM10. Periods of low precipitation were consistently associated with higher concentrations of these pollutants, highlighting the importance of wet scavenging as an effective removal mechanism for both gaseous and particulate pollutants [22,44]. This effect is particularly pronounced for particulate matter, where rainfall events can rapidly reduce ambient concentrations through washout processes [14]. The results emphasize the need to consider precipitation variability when interpreting trends in air quality data or designing mitigation strategies.

Humidity demonstrated pollutant-specific effects. For NO, NO_2, PM2.5, CO, and PM10, higher humidity was generally associated with increased concentrations. This may be attributed to enhanced secondary formation processes, such as the aqueous-phase production of secondary aerosols or the hygroscopic growth of particles [14,44]. In contrast, for O_3, lower humidity was linked to higher concentrations, possibly due to reduced ozone destruction via titration with water vapor or other humidity-dependent chemical pathways [23]. These divergent effects highlight the complex interplay between humidity and atmospheric chemistry in urban environments.

Atmospheric pressure was consistently identified as a positive driver for all pollutants studied. High-pressure systems are typically associated with stable atmospheric conditions, reduced vertical mixing, and limited dispersion, all of which facilitate the accumulation of pollutants near the surface. This finding aligns with the well-documented phenomenon of pollution episodes during stagnant, high-pressure weather patterns [14,22].

Wind speed exhibited a clear and consistent inverse relationship with pollutant concentrations. Lower wind speeds were associated with higher levels of all pollutants, reflecting the fundamental role of atmospheric dispersion in diluting and transporting air pollutants away from their sources. This effect was particularly notable for primary pollutants such as NO and CO, as well as for particulate matter, where stagnant conditions can lead to substantial accumulation [22,44].

Solar radiation was found to be a unique and important driver for O_3, with higher radiation levels promoting increased ozone concentrations. This is consistent with the photochemical nature of ozone formation, which depends on the availability of sunlight to drive the necessary chemical reactions involving precursor gases such as nitrogen oxides and volatile organic compounds [23,37].

In summary (Table 4), the SHAP analysis reveals both shared and pollutant-specific meteorological drivers of urban air quality. Temperature and pressure are the most universally influential variables, while precipitation and humidity show more nuanced, pollutant-dependent effects. The results underscore the importance of accounting for meteorological variability in air quality management, forecasting, and policy development [22,44]. By quantifying the meteorological contributions to each pollutant, this study provides a robust scientific basis for targeted mitigation strategies and supports the development of more accurate air quality models for urban environments. These insights are crucial for understanding the physical processes governing air pollution and for designing effective interventions to protect public health in cities like Stuttgart [14,47].

Table 4. Comparative summary table.

Pollutant	Most Influential Meteorological Factors	Direction of Influence (High Value)
NO	Temperature, Humidity, Pressure, Wind Speed	↑ Temperature, ↑ Humidity, ↑ Pressure, ↓ Wind Speed
NO_2	Temperature, Precipitation, Pressure, Humidity, Wind Speed	↑ Temperature, ↓ Precipitation, ↑ Pressure, ↑ Humidity, ↓ Wind Speed
O_3	Temperature, Humidity, Radiation, Pressure, Wind Speed	↑ Temperature, ↓ Humidity, ↑ Radiation, ↑ Pressure, (Mixed) Wind Speed
PM2.5	Temperature, Precipitation, Pressure, Humidity, Wind Speed	↑ Temperature, ↓ Precipitation, ↑ Pressure, ↑ Humidity, ↓ Wind Speed
CO	Temperature, Humidity, Pressure, Wind Speed	↑ Temperature, ↑ Humidity, ↑ Pressure, ↓ Wind Speed
PM10	Temperature, Precipitation, Pressure, Humidity, Wind Speed	↑ Temperature, ↓ Precipitation, ↑ Pressure, ↑ Humidity, ↓ Wind Speed

Note: ↑ indicates that higher values of the meteorological variable are associated with higher pollutant concentrations, while ↓ indicates that higher values of the meteorological variable are associated with lower pollutant concentrations. "Mixed" denotes a variable showing both positive and negative influences depending on conditions.

3.5. Directional Distribution Patterns of Primary Pollutants

Carbon Monoxide and Nitrogen Oxide Source Signatures

Wind rose analyses revealed pronounced directional clustering of carbon monoxide (CO) and nitrogen oxide (NO) concentrations, with peak values (>394.5 $\mu g/m^3$ CO; >31.4 $\mu g/m^3$ NO) predominantly associated with southern and southeastern wind sectors (Figure A3a,b). These sectors accounted for 7–8% of total observations, indicating localized emission sources aligned with Stuttgart's major traffic corridors, including the B14 and B27 highways. The narrow angular distribution of elevated concentrations (227.4–338.8 $\mu g/m^3$ CO; 6.5–19.0 $\mu g/m^3$ NO) suggests proximal linear emission sources rather than diffuse urban background contributions. The parallel behaviour between

CO and NO, both primary combustion byproducts, confirms vehicular exhaust as their dominant shared source, consistent with Stuttgart's traffic density patterns [14,35,39].

Ozone (O_3) concentrations displayed a multi-directional profile, with maxima (>45.6 $\mu g/m^3$) occurring under western and southwestern winds (Figure A3c). These sectors correspond to synoptic-scale airflow transporting ozone-rich air from the Upper Rhine Valley, where precursor emissions (NO_x, VOCs) from industrial and agricultural sources undergo photochemical processing. Local O_3 production in southern sectors (36.8–45.6 $\mu g/m^3$) occurred during stagnant conditions, driven by in situ NO_2 photolysis under high solar irradiance. The anticorrelation between O_3 and NO_2 in southern quadrants ($r = -0.72$, $p < 0.01$) confirms titration dynamics, where fresh NO emissions rapidly scavenge O_3 [37,39].

Nitrogen dioxide (NO_2) exhibited a distinct bimodal distribution, with primary peaks in southern sectors (25.1–45.6 $\mu g/m^3$) and secondary maxima in western directions (19.9–25.1 $\mu g/m^3$) as shown in Figure A3d. The southern component aligns with local NO oxidation from vehicular NO emissions, while the western signal correlates with regional transport of aged air masses containing secondary NO_2. This dual origin is reinforced by NO_2's longer atmospheric lifetime (hours to days) compared to NO (minutes), enabling both local photochemical production and advection from Stuttgart's industrial periphery [14,37].

Particulate matter concentrations PM10 and PM2.5 (Figure A3e,f) exhibited nearly identical directional patterns, with 68% of peak concentrations (>27.4 $\mu g/m^3$ for PM10 and >21.8 $\mu g/m^3$ for PM2.5) originating from southern wind directions (Table A4), indicating shared emission sources that include primary diesel vehicle exhaust emissions (predominantly contributing to PM2.5), secondary aerosol formation through sulphate and nitrate production from SO_2 and NO_x precursors (contributing to PM10), and mechanical resuspension of road dust generated by vehicular traffic (contributing to PM10) [14,34,38]. The notable absence of elevated particulate matter concentrations from western wind directions, despite the presence of regional NO_2 signals from this sector, suggests significant particulate deposition occurs during atmospheric transport, contrasting markedly with the persistence characteristics of gaseous NO_2 species during similar transport conditions [14].

3.6. Implications for Air Quality Management

The spatial analysis reveals that the consistent southern clustering of CO, NO, and PM concentrations may reflect the influence of nearby traffic corridors and local street-canyon characteristics around Marienplatz. While these findings suggest that traffic emissions may contribute significantly to pollutant levels in this area, they should be interpreted as site-specific and not necessarily representative of conditions across all districts of Stuttgart. Nevertheless, previous modeling studies have suggested that diverting approximately 40% of B14 highway traffic could potentially reduce PM2.5 and NO_2 concentrations by about 23–29%, highlighting the possible benefits of targeted traffic management measures in heavily trafficked corridors [14,39]. Furthermore, the observed western components of NO_2 and O_3 distributions necessitate cross-jurisdictional coordination strategies, particularly with Baden-Württemberg's industrial zones, where implementing VOC controls in the Mannheim/Ludwigshafen region could achieve 12–18% reductions in Stuttgart's peak O_3 concentrations under westerly flow regimes [37,38]. However, current wind rose methodologies present inherent limitations in discriminating between source types (diesel versus gasoline vehicles), vertical mixing effects, and temporal variations (diurnal and seasonal patterns), highlighting the need for future research integration of chemical speciation through Positive Matrix Factorization (PMF) analysis of particulate matter components, vertical profiling using Light Detection and Ranging (LiDAR) measurements of boundary

layer dynamics, and development of high-resolution emission inventories incorporating detailed traffic and industrial source databases to enhance the precision and applicability of pollution source identification and mitigation strategies [14].

This analysis provides a spatially resolved foundation for Stuttgart's 2030 Air Quality Action Plan, prioritizing targeted local measures while advocating for regional policy integration [14]. The integration of explainable machine learning with directional source analysis demonstrated in this study provides a transferable methodological framework for other urban environments seeking to distinguish local emission changes from meteorological variability in long-term air quality datasets.

4. Conclusions and Policy Implications

This multi-year, multi-method analysis examines air quality at the Marienplatz monitoring station in Stuttgart, an urban street-canyon site strongly influenced by local traffic patterns and complex surrounding geometry. The results demonstrate that pandemic-induced reductions in anthropogenic activity led to immediate and substantial decreases in primary traffic-related pollutants, particularly CO, NO, and NO_2. However, reduced data completeness for certain pollutants in later years (particularly PM and CO) introduces additional uncertainty in the interpretation of long-term trends, and these results should therefore be interpreted with appropriate caution. By integrating meteorological normalization, explainable machine-learning attribution (SHAP), and directional wind-based source diagnostics, this study provides a comprehensive framework for disentangling emission-driven and meteorologically driven changes in urban air quality.

The application of meteorological normalization together with machine learning-based feature attribution indicates that these improvements were largely associated with emission reductions rather than favourable weather conditions. However, the observed increases in ozone concentrations during and after the lockdown periods underscore the complexity of urban atmospheric chemistry, wherein reductions in NO_x emissions can inadvertently enhance photochemical ozone production due to shifts toward NO_x-sensitive regimes. Particulate matter levels, especially PM2.5 and PM10, demonstrated relative insensitivity to short-term traffic interventions, highlighting the significance of non-traffic sources and regional transport in sustaining urban particulate burdens. The persistence of altered photochemical regimes and emission patterns in the post-lockdown years indicates that urban atmospheric systems may not rapidly revert to pre-pandemic baselines, and that lasting behavioural and structural changes can have enduring effects on air quality. The findings of this study have several critical implications for urban air quality management and policy development:

(a) Multi-Pollutant, Multi-Sectoral Strategies: Effective air quality improvement requires integrated approaches targeting both primary and secondary pollutants. Policies should not only focus on traffic emissions but also address residential heating, industrial sources, and regional pollutant transport.
(b) Dynamic Emission Controls: The transient nature of air quality improvements during the lockdown highlights the need for sustained and adaptive emission reduction measures, including the expansion of low-emission zones, electrification of transport fleets, and promotion of clean heating technologies.
(c) Photochemical Regime Sensitivity: The observed enhancement of ozone formation efficiency during periods of reduced NO_x emissions underscores the necessity of coordinated NO_x and VOC control strategies, particularly under warming climate scenarios that favour higher ozone production.
(d) Meteorologically Informed Management: The observed association between higher temperatures and elevated ozone concentrations suggests that air quality forecasting

and public health advisories should be dynamically linked to meteorological and climate projections, enabling timely interventions during high-risk periods.

(e) Regional and Cross-Jurisdictional Coordination: The influence of regional transport on NO_2 and O_3 concentrations necessitates collaborative policy frameworks that transcend municipal boundaries, particularly for managing transboundary ozone and precursor emissions.

(f) Continuous Monitoring and Research: Ongoing high-resolution monitoring, advanced source apportionment, and atmospheric modelling are essential for tracking evolving emission patterns, detecting changes in photochemical regimes, and evaluating the real-time effectiveness of policy interventions.

In summary, the COVID-19 pandemic has provided an unprecedented natural experiment that offered valuable insights into the responsiveness of urban air quality to rapid emission changes. These findings should inform the development of resilient, science-based air quality and climate policies capable of delivering sustained public health and environmental benefits in Stuttgart and potentially informing air-quality management strategies in other urban environments with similar characteristics.

Outlook on Future Regulations

Although this study evaluated air quality trends against current EU regulatory standards, it is important to acknowledge that new, more stringent limit values will be implemented in 2030. While exceedances at Marienplatz were rare or minimal under existing standards, the application of these future regulations could alter the compliance status and underscore new challenges for air quality management in Stuttgart. This forward-looking perspective reinforces the need for adaptive policy measures and continuous assessment as regulatory benchmarks evolve.

Author Contributions: Conceptualization, A.S. and U.V.; methodology, A.S., M.N. and G.O.; validation, A.S.; formal analysis, M.N.; investigation, A.S. and M.N.; resources, U.V.; data curation, M.N. and F.N.; writing—original draft preparation, A.S. and M.N.; writing—review and editing, A.S., M.N., G.O. and U.V.; visualization, F.N.; software, F.N.; supervision, A.S. and U.V.; project administration, U.V.; funding acquisition, U.V. All authors have read and agreed to the published version of the manuscript.

Funding: This work was funded by the Federal Ministry of Education and Research (BMBF), Germany. Funding number: 01LP1912.

Data Availability Statement: The data presented in this study are available on request from the corresponding author due to privacy.

Acknowledgments: This work was performed under the project Urban Climate Under Change. The authors thank the project partners for their support.

Conflicts of Interest: Mr. Macdonald Nwamuo is an employee of Spiraltec GmbH. The company had no roles in the design of the study; in the collection, analysis, or interpretation of data; in the writing of the manuscript, or in the decision to publish the articles. The paper reflects the views of the scientists and not the company.

Appendix A

Table A1. Air quality monitoring devices deployed in Stuttgart's Marienplatz, Germany.

Instrument	Measuring Principle	Measured Parameters	Accuracy	Resolution
Environmental Dust Monitor, EDM180 (Aerosol spectrometer)	Light scattering	Particulate Matter (PM) with a size range of 0.25–32 µm	5%	0.1 µg/m^3
NO_2/NO/NO_X monitor, MLU200a	Chemiluminescence	NO_2, NO, NO_X	0.5%	0.1 ppb
Ozone Monitor, HORIBA APOA 360	UV absorption	O_3	2%	0.1 ppb
CO monitor, HORIBA APMA 360	NDIR absorption	CO	1%	0.1 ppm

Table A2. Meteorological measurement devices at Marienplatz, Stuttgart, Germany.

Instrument	Measuring Principle	Measured Parameter	Accuracy	Resolution
Weather station	Negative Temperature Coefficient (NTC) resistor	Air temperature	0.5 °C	0.1 °C
	Capacitive humidity sensor	Relative humidity	5%	0.1%
	Micro Electro-Mechanical Sensor (MEMS)	Atmospheric pressure	1.5 hPa	0.1 hPa
	Pyranometer	Global radiation	2%	1 W/m^2
Wind sensor	Ultrasonic time of flight	Wind speed	0.2 m/s	0.2 m/s
	Ultrasonic time of flight	Wind direction	10 °	0.5 °
Precipitation sensor	Tipping bucket system	Precipitation intensity	2%	2 cm^3

Table A3. Summary of raw and meteorologically adjusted trends for key pollutants (2018–2022), Marienplatz, Stuttgart.

Pollutant	Pre-Lockdown and Post-Lockdown Raw Trend (2018–2022)	Adjusted Trend (2018–2022)	Meteorological Influence	Main Drivers of Change	Policy Implications
CO		Could not be determined due to insufficient dataset			
NO	Decrease (11.6 → 8.0 µg/m^3) −31.0%	Decrease (10.1 → 9.6 µg/m^3) −4.8%	Moderate negative correlation with temperature (r = −0.32, R^2 = 0.10) and wind speed (r = −0.25, R^2 = 0.06)	Clear traffic reduction signal: Lockdown −4.8%, sustained post-lockdown −5.4% (90% traffic sensitivity).	Strong evidence for traffic policy: Most traffic-sensitive pollutant. Continue/reinforce traffic reduction measures.
NO_2	Decrease (35.6 → 30.0 µg/m^3) −15.7%	Minimal decrease (33.9 → 33.1 µg/m^3) −2.2%	Moderate negative correlation with temperature (r = −0.29, R^2 = 0.09) and wind speed (r = −0.23, R^2 = 0.05)	Meteorology explains most raw trend: Only −2.2% true reduction despite 80% traffic sensitivity.	Traffic benefits limited: Raw data overstates improvements. Need complementary NOx reduction strategies beyond traffic.

Table A3. *Cont.*

Pollutant	Pre-Lockdown and Post-Lockdown Raw Trend (2018–2022)	Adjusted Trend (2018–2022)	Meteorological Influence	Main Drivers of Change	Policy Implications
O_3	Increase (48.5 → 68.4 μg/m^3) +41.0%	Stable (58.1 → 58.7 μg/m^3) +1.1%	Extremely strong positive correlation with temperature (r = 0.56, R^2 = 0.32) and radiation (r = 0.36, R^2 = 0.13)	Purely meteorological: Negative traffic sensitivity (−30%) means reduced traffic should increase O_3, but normalized data shows no lockdown effect.	Climate-driven policy: O_3 control = climate adaptation. Focus on VOC controls alongside NOx to avoid titration loss.
PM2.5	Fluctuating (9.0 → 9.5 μg/m^3) +5.6%	Decrease (9.6 → 9.3 μg/m^3) −3.1%	Very weak influence: pressure strongest (r = 0.22, R^2 = 0.05), all R^2 < 0.05	Mixed sources: 50% traffic sensitivity but lockdown reduction small (−2.5%). Post-lockdown continued improvement (−3.1%)	Broad approach needed: Traffic contributes but not dominant. Target other sources: residential combustion, industry, secondary formation
PM10	Increase (11.0 → 12.2 μg/m^3) +10.9%	Stable (12.4 → 12.3 μg/m^3) −0.8%	Very weak influence: pressure strongest (r = 0.25, R^2 = 0.06), all R^2 < 0.06	Meteorology masks stability: 60% traffic sensitivity but lockdown shows +1.0% normalized increase. Post-lockdown −1.0%.	Non-traffic focus: Resuspension, construction dust, long-range transport. Limited traffic control effectiveness.

Note: "→" indicates the change from the initial to the final concentration value.

Table A4. Key findings summary.

Pollutant	Primary Direction	Key Process	Mitigation Strategy
CO/NO	South/Southeast	Vehicular combustion	Traffic electrification
NO_2	South + West	Local oxidation + regional transport	VOC controls in industrial zones
O_3	West/Southwest	Regional photochemistry	Cross-state emission caps
PM10/PM2.5	South	Resuspension + primary emissions	Road surface cleaning

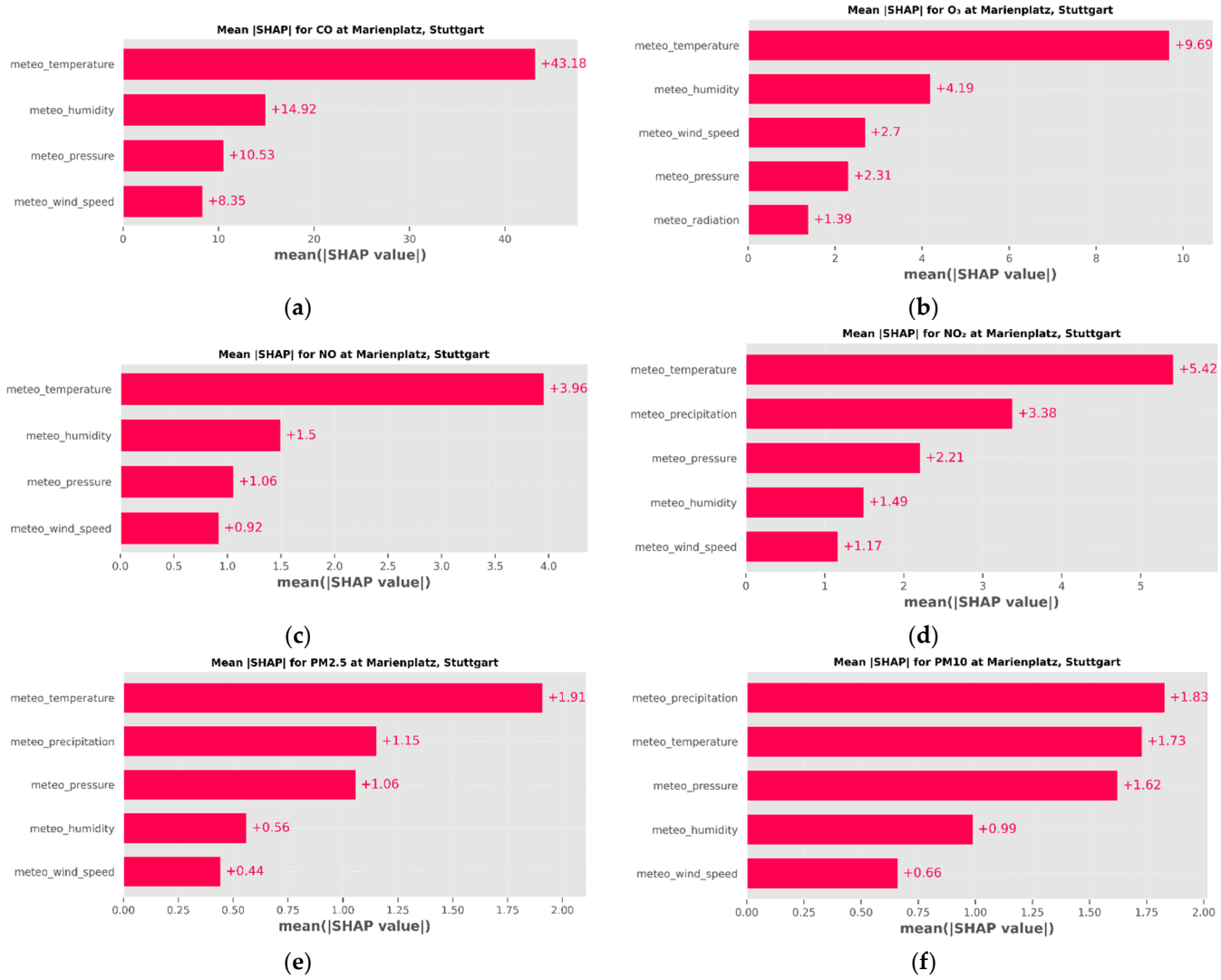

Figure A1. Mean absolute SHAP bar plot values for key meteorological variables influencing the air pollutant concentrations at Marienplatz, Stuttgart. (**a**) Mean absolute SHAP values for meteorological predictors (temperature, humidity, pressure, wind patterns) influencing CO concentrations, ranked by their contribution to the model output. (**b**) Mean absolute SHAP values for compensation and background predictors influencing O_3 formation, ranked by their contribution to the model output. (**c**) Mean absolute SHAP values for manufacturing and process-related features influencing NO concentrations, ranked by their contribution to the model output. (**d**) Mean absolute SHAP values for temporal and network factors influencing NO_2 concentrations, ranked by their contribution to the model output. (**e**) Mean absolute SHAP values for median-based and structural predictors influencing PM2.5 concentrations, ranked by their contribution to the model output. (**f**) Mean absolute SHAP values for media and contribution-related features influencing PM10 concentrations, ranked by their contribution to the model output.

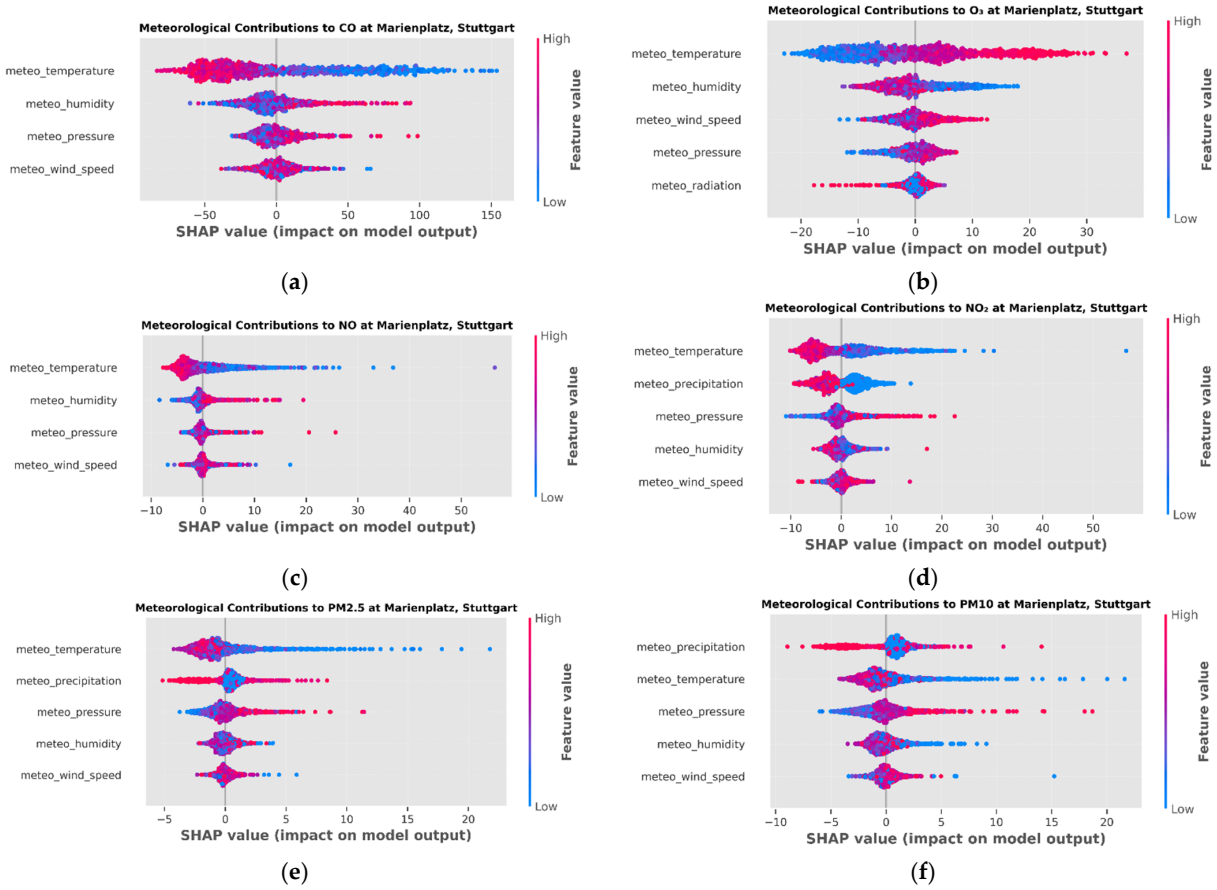

Figure A2. SHAP summary plots values for key meteorological variables influencing the air pollutant concentrations at Marienplatz, Stuttgart. (**a**) Meteorological predictors for CO. (**b**) Network-related predictors for O_3. (**c**) Precipitation and wind speed predictors for NO. (**d**) Temperature and radiation predictors for NO_2. (**e**) Pressure and soil-related predictors for PM2.5. (**f**) Meteorological initialization predictors for PM10.

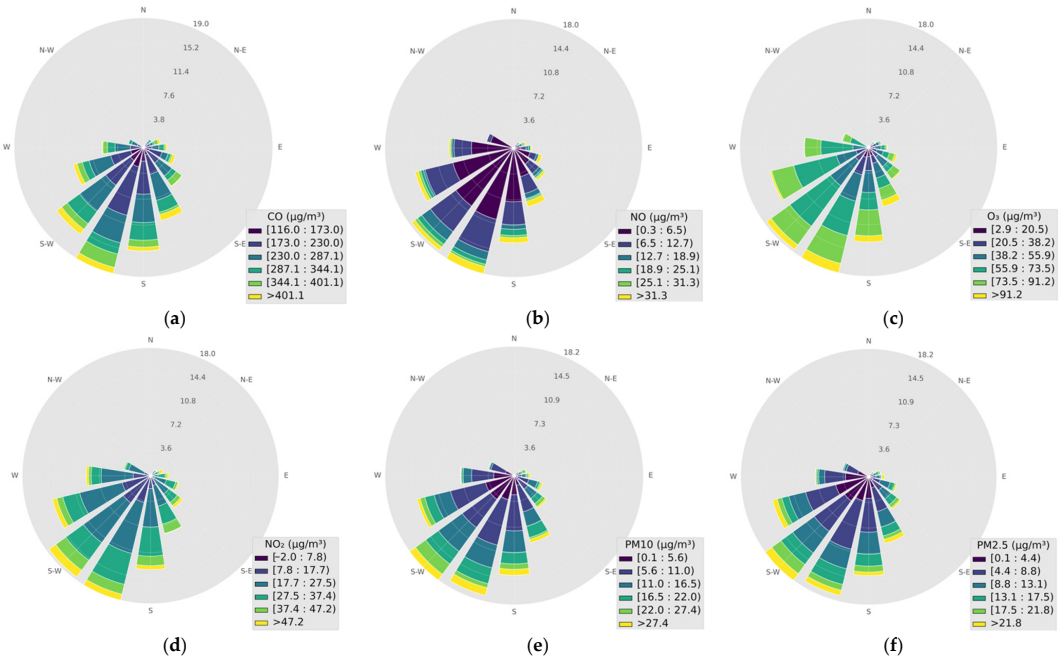

Figure A3. Wind roses showing the distribution of pollutant concentrations by wind speed and direction ($\mu g/m^3$) at Marienplatz, Stuttgart. (**a**) CO. (**b**) NO. (**c**) O_3. (**d**) NO_2. (**e**) PM10. (**f**) PM2.5.

References

1. World Health Organization. WHO Global Air Quality Guidelines. 2021. Available online: https://www.who.int/publications/i/item/9789240034228 (accessed on 23 April 2025).
2. Landrigan, P.J.; Fuller, R.; Acosta, N.J.; Adeyi, O.; Arnold, R.; Basu, N.N.; Baldé, A.B.; Bertollini, R.; Bose-O'Reilly, S.; Boufford, J.I.; et al. The lancet commission on pollution and health. *Lancet* **2018**, *391*, 462–512. [CrossRef]
3. Gurjar, B.R.; Ravindra, K.; Nagpure, A.S. Air pollution trends over Indian megacities and their local-to-global implications. *Atmos. Environ.* **2016**, *142*, 475–495. [CrossRef]
4. Balakrishnan, K.; Dey, S.; Gupta, T.; Dhaliwal, R.S.; Brauer, M.; Cohen, A.J.; Stanaway, J.D.; Beig, G.; Joshi, T.K.; Dandona, L.; et al. The impact of air pollution on deaths, disease burden, and life expectancy across the states of India: The Global Burden of Disease Study 2017. *Lancet Planet. Health* **2019**, *3*, e26–e39. [CrossRef]
5. European Environment Agency. Air Quality in Europe, 2020 Report (Report No. 09/2020). Publications Office of the European Union. 2020. Available online: https://op.europa.eu/en/publication-detail/-/publication/447035cd-344e-11eb-b27b-01aa75ed71a1/language-en (accessed on 21 August 2025).
6. Anenberg, S.C.; Mohegh, A.; Goldberg, D.L.; Kerr, G.H.; Brauer, M.; Burkart, K.; Hystad, P.; Larkin, A.; Wozniak, S.; Lamsal, L. Long-term trends in urban NO_2 concentrations and associated paediatric asthma incidence: Estimates from global datasets. *Lancet Planet. Health* **2022**, *6*, e49–e58. [CrossRef]
7. Kumar, P.; Morawska, L.; Martani, C.; Biskos, G.; Neophytou, M.; Di Sabatino, S.; Bell, M.; Norford, L.; Britter, R. The rise of low-cost sensing for managing air pollution in cities. *Environ. Int.* **2015**, *75*, 199–205. [CrossRef] [PubMed]
8. Snyder, E.G.; Watkins, T.H.; Solomon, P.A.; Thoma, E.D.; Williams, R.W.; Hagler, G.S.W.; Shelow, D.; Hindin, D.A.; Kilaru, V.J.; Preuss, P.W. The changing paradigm of air pollution monitoring. *Environ. Sci. Technol.* **2013**, *47*, 11369–11377. [CrossRef]
9. Creutzig, F.; Jochem, P.; Edelenbosch, O.Y.; Mattauch, L.; van Vuuren, D.P.; McCollum, D.; Minx, J. Transport: A roadblock to climate change mitigation? *Science* **2015**, *350*, 911–912. [CrossRef]
10. Brand, C. Beyond 'Dieselgate': Implications of unaccounted and future air pollutant emissions and energy use for cars in the United Kingdom. *Energy Policy* **2016**, *97*, 1–12. [CrossRef]
11. Janssen, N.A.H.; Hoek, G.; Simic-Lawson, M.; Fischer, P.; van Bree, L.; ten Brink, H.; Keuken, M.; Atkinson, R.W.; Anderson, H.R.; Brunekreef, B.; et al. Black carbon as an additional indicator of the adverse health effects of airborne particles compared with PM10 and PM2.5. *Environ. Health Perspect.* **2012**, *120*, 708–714. [CrossRef]
12. Jacob, D.J.; Winner, D.A. Effect of climate change on air quality. *Atmos. Environ.* **2009**, *43*, 51–63. [CrossRef]
13. European Union. Directive 2008/50/EC of the European Parliament and of the Council of 21 May 2008 on ambient air quality and cleaner air for Europe. *Off. J. Eur. Union L* **2008**, *152*, 1–44. Available online: https://eur-lex.europa.eu/eli/dir/2008/50/oj (accessed on 21 August 2025).
14. European Environment Agency. Air Quality in Europe, 2021 Report (Report No. 15/2021). Publications Office of the European Union. 2021. Available online: https://www.eea.europa.eu/publications/air-quality-in-europe-2021 (accessed on 30 September 2025).
15. European Union. Directive (EU) 2024/1203 of the European Parliament and of the Council of 24 April 2024 on Ambient Air Quality and Cleaner Air for Europe and Repealing Directive 2008/50/EC and Directive 2004/107/EC*. Official Journal of the European Union, L 2024/1203. 2024. Available online: https://eur-lex.europa.eu/eli/dir/2024/1203/oj (accessed on 30 September 2025).
16. German Environment Agency. Air Quality 2020: Only a Few Cities Still Exceed Nitrogen Dioxide Limit [Press Release]. Available online: https://www.umweltbundesamt.de/en/press/pressinformation/air-quality-2020-only-a-few-cities-still-exceed (accessed on 16 February 2025).
17. Bundesministerium für Umwelt; Naturschutz und Nukleare Sicherheit. Umweltpolitik für eine Nachhaltige Gesellschaft: Nachhaltigkeitsbericht des Bundesumweltministeriums zur Umsetzung der 2030-Agenda der Vereinten Nationen. 2020. Available online: https://www.bundesregierung.de/resource/blob/2196306/1804738/ad27f57b2d79d245c53ad1af3a19f8b3/2020-bmu-bericht-nachhaltigkeit-10-2020-data.pdf?download=1 (accessed on 3 November 2025).
18. Umweltbundesamt. Jahresbericht Luftqualität 2021 [Annual Air Quality Report 2021]. 2022. Available online: https://www.umweltbundesamt.de/publikationen/luftqualitaet-2021 (accessed on 12 December 2025).
19. Lenschow, P.; Abraham, H.J.; Kutzner, K.; Lutz, M.; Preuß, J.D.; Reichenbächer, W. Some ideas about the sources of PM10. *Atmos. Environ.* **2001**, *35*, S23–S33. [CrossRef]
20. Regierungspräsidium Stuttgart. Luftreinhalteplan für den Regierungsbezirk Stuttgart: Teilplan Landeshauptstadt Stuttgart—5. Fortschreibung des Luftreinhalteplans zur Minderung der NO_2-Belastung (März 2020). 2020. Available online: https://www.stuttgart.de/medien/ibs/Luftreinhalteplan-fuer-den-Regierungsbezirk-Stuttgart-Teilplan-Landeshauptstadt-Stuttgart.pdf (accessed on 3 November 2025).

21. Bauwens, M.; Compernolle, S.; Stavrakou, T.; Müller, J.-F.; van Gent, J.; Eskes, H.; Levelt, P.F.; van der Veefkind, J.P.A.R.; Vlietinck, J.; Yu, H.; et al. Impact of coronavirus outbreak on NO_2 pollution assessed using TROPOMI and OMI observations. *Geophys. Res. Lett.* **2020**, *47*, e2020GL087978. [CrossRef]
22. Petetin, H.; Bowdalo, D.; Soret, A.; Guevara, M.; Jorba, O.; Serradell, K.; Pérez García-Pando, C. Meteorology-normalized impact of the COVID-19 lockdown upon NO_2 pollution in Spain. *Atmos. Chem. Phys.* **2020**, *20*, 11119–11141. [CrossRef]
23. Sicard, P.; De Marco, A.; Agathokleous, E.; Feng, Z.; Xu, X.; Paoletti, E.; Rodriguez, J.J.D.; Calatayud, V. Amplified ozone pollution in cities during the COVID-19 lockdown. *Sci. Total Environ.* **2020**, *735*, 139542. [CrossRef]
24. Schäfer, K.; Wagner, P.; Emeis, S.; Kramar, J. Post-lockdown changes in air quality trends in Stuttgart, Germany. *Atmos. Environ.* **2021**, *256*, 118460. [CrossRef]
25. Kühlwein, J.; Friedrich, R.; Wickert, B. Luftqualität Während der COVID-19-Pandemie in Baden-Württemberg [Air Quality During the COVID-19 Pandemic in Baden-Württemberg]. Landesanstalt für Umwelt Baden-Württemberg. 2020. Available online: https://www.lubw.baden-wuerttemberg.de (accessed on 12 December 2025).
26. Baden-Württemberg State Statistical Office. Statistisches Jahrbuch Baden-Württemberg 2023 [Statistical Yearbook of Baden-Württemberg 2023]. 2023. Available online: https://www.statistik-bw.de (accessed on 9 May 2025).
27. Stuttgart City. About Stuttgart. Available online: https://stuttgart.city/about/ (accessed on 28 May 2025).
28. Verband Region Stuttgart. Einwohner und Fläche. 2023. Available online: https://www.region-stuttgart.org/de/verband/region-in-zahlen/einwohner-und-flaeche/ (accessed on 25 May 2025).
29. Samad, A.; Vogt, U. Assessing the effect of traffic density and cold airflows on the urban air quality of a city with complex topography using continuous measurements. *Mod. Environ. Sci. Eng.* **2020**, *6*, 529–541. [CrossRef]
30. European Environment Agency. Stuttgart: Combating the Heat Island Effect and Poor Air Quality with Green Ventilation Corridors (Climate ADAPT Case Study). Climate ADAPT. 2020. Available online: https://climate-adapt.eea.europa.eu/en/metadata/case-studies/stuttgart-combating-the-heat-island-effect-and-poor-air-quality-with-green-ventilation-corridors (accessed on 9 February 2026).
31. Landeshauptstadt Stuttgart. Air Quality in Stuttgart: Monitoring and Long-Term Measurements. City of Stuttgart. 2024. Available online: https://www.stuttgart.de/leben/umwelt/luft (accessed on 15 July 2025).
32. Stadtklima Stuttgart. The Air in Stuttgart [Dataset]. 2021. Available online: https://www.stadtklima-stuttgart.de/index.php?luft_messdaten_stationen_in_stuttgart (accessed on 17 April 2025).
33. German Federal Ministry of Education and Research; BMBF. Urban Climate Under Change $[UC]^2$ Research Initiative. 2017. Available online: https://www.bmbf.de (accessed on 15 December 2025).
34. Collivignarelli, M.C.; Abbà, A.; Bertanza, G.; Pedrazzani, R.; Ricciardi, P.; Carnevale Miino, M. Lockdown for COVID-19 in Milan: What are the effects on air quality? *Sci. Total Environ.* **2020**, *732*, 139280. [CrossRef]
35. Dantas, G.; Siciliano, B.; França, B.B.; da Silva, C.M.; Arbilla, G. The impact of COVID-19 partial lockdown on the air quality of the city of Rio de Janeiro, Brazil. *Sci. Total Environ.* **2020**, *729*, 139085. [CrossRef]
36. Venter, Z.S.; Aunan, K.; Chowdhury, S.; Lelieveld, J. COVID-19 lockdowns cause global air pollution declines with implications for public health risk. *medRxiv* **2020**. [CrossRef]
37. Grange, S.K.; Lee, J.D.; Drysdale, W.S.; Lewis, A.C.; Hueglin, C.; Emmenegger, L.; Carslaw, D.C. COVID-19 lockdowns highlight a risk of increasing ozone pollution in European urban areas. *Atmos. Chem. Phys.* **2021**, *21*, 4169–4185. [CrossRef]
38. Menut, L.; Bessagnet, B.; Siour, G.; Mailler, S.; Pennel, R.; Cholakian, A. Impact of lockdown measures to combat COVID-19 on air quality over western Europe. *Sci. Total Environ.* **2020**, *741*, 140426. [CrossRef]
39. Baldasano, J.M. COVID-19 lockdown effects on air quality by NO_2 in the cities of Barcelona and Madrid (Spain). *Sci. Total Environ.* **2020**, *741*, 140353. [CrossRef]
40. Shi, X.; Brasseur, G.P. The response in air quality to the reduction of Chinese economic activities during the COVID-19 outbreak. *Geophys. Res. Lett.* **2020**, *47*, e2020GL088070. [CrossRef]
41. Sillman, S. The relation between ozone, NOx, and hydrocarbons in urban and polluted rural environments. *Atmos. Environ.* **1999**, *33*, 1821–1845. [CrossRef]
42. Seinfeld, J.H.; Pandis, S.N. *Atmospheric Chemistry and Physics: From Air Pollution to Climate Change*, 3rd ed.; Wiley: Hoboken, NJ, USA, 2016.
43. Monks, P.S.; Archibald, A.T.; Colette, A.; Cooper, O.; Coyle, M.; Derwent, R.; Fowler, D.; Granier, C.; Law, K.S.; Mills, G.; et al. Tropospheric ozone and its precursors from the urban to the global scale. *Atmos. Chem. Phys.* **2015**, *15*, 8889–8973. [CrossRef]
44. Grange, S.K.; Lewis, A.C.; Moller, S.J.; Carslaw, D.C. Lower vehicular emissions during COVID-19 lockdowns: A review of published evidence and implications for future urban air quality policy. *Environ. Sci. Process. Impacts* **2018**, *22*, 1805–1816.
45. Petetin, H.; Bowdalo, D.; Soret, A.; Guevara, M.; Jorba, O.; Serradell, K.; Pérez García-Pando, C. Meteorology-driven variability of air pollution (PM_1) revealed with explainable machine learning. *Atmos. Chem. Phys.* **2021**, *21*, 3919–3948. [CrossRef]

46. Lundberg, S.M.; Lee, S.I. A unified approach to interpreting model predictions. *Adv. Neural Inf. Process. Syst.* **2017**, *30*, 4765–4774.
47. Sicard, P.; Agathokleous, E.; De Marco, A.; Paoletti, E.; Calatayud, V. Urban air pollution trends and climate interactions: A European perspective. *Sci. Total Environ.* **2022**, *827*, 154275. [CrossRef]